Check for updates

Angewandte Chemie International Edition

Angewandte International Edition Chemie

How to cite: *Angew. Chem. Int. Ed.* **2026**, 65, e6667904
doi.org/10.1002/anie.6667904

RESEARCH ARTICLE OPEN ACCESS

1,7-Digallatetracarborane: Between Nucleophilic *closo*-Cluster and "Inverse Sandwich" Digallylene

Julijan Sarcevic[1] | Tobias Heitkemper[1] | Niklas Mehner[1] | Maximilian Kubis[2] | Christian P. Sindlinger[1]

[1]Institut für Anorganische Chemie, Universität Stuttgart, Stuttgart, Germany | [2]Institut für Anorganische Chemie, RWTH Aachen University, Aachen, Germany

Correspondence: Christian P. Sindlinger (christian.sindlinger@iac.uni-stuttgart.de)

Received: 4 March 2026 | **Revised:** 15 April 2026 | **Accepted:** 21 April 2026

Keywords: borole | carborane clusters | gallium | main group chemistry | sandwich compounds

ABSTRACT

This manuscript describes the synthesis and chemistry of an unprecedented carborane cluster of low-valent main-group elements with a unique structural motif. On the basis of a dianionic borole π-ligand platform (L = $[R_5(C_4B)]^{2-}$) an "inverse sandwich", Janus-type digallylene complex $L(Ga^{+I})_2$ featuring two nucleophilic Ga(I) ions was accessed. This compound can also be described as a *closo*-type 1,7-digallatetracarborane cluster. Preliminary reactivity studies on this new compound class have been conducted. Assessment of Lewis-basicity in coordination chemistry with transition metals and main group Lewis-acids indicate electronic communication between the Ga-atoms. Oxidation with free borole (L) gives rise to bent digallocene $L(Ga^{+II})$–$(Ga^{+II})L$, the first group 13 element-based dimetallocene-type compound. Examples demonstrate that $L(Ga^{+I})_2$ can behave as both a discrete digallacarborane cluster and a bis-gallylene π-complex capable of releasing Ga^+.

1 | Introduction

The cyclopentadienyl ligand (Cp^-) has been instrumental in the early developments of low-valent main group organometallic species. Cp^- and its respective substituted derivatives $(Cp^R)^-$ allowed breakthrough discoveries and isolations of a number of fundamental low-valent main group species [1–11]. This is due to the ligand's robustness caused by the effective delocalization of anionic charge, its tunable steric profile occupying a fair share of a half-sphere around a respective bound atom, and its propensity to serve both as a σ- as well as a π−donor. Respective main group element (E) derivatives $[(Cp^R)_nE]$ reveal a rich chemistry with regard to reactivity toward small molecules or applicability as metal-centered donor ligands in coordination chemistry [12–14]. Over the years, by isoelectronic replacement of one or more carbon atoms with main group elements, a plethora of metallolyl derivatives more or less mimicking the electronic structure of Cp^- have been synthetically accessed and often successfully applied in coordination chemistry. For example, a rich chemistry of tetreloles ($[(RC)_4ER']^-$ or $[(RC)_4E]^{2-}$ E = Si-Pb) has been developed [15–20].

Respective five-membered (multi-)anionic π-ligands containing boron have been extensively studied over the years. Ligand platforms of this type span a wide chemical range that progressively transitions with increasing boron content from discrete heterocycles such as boroles (C_4B), diboroles (C_3B_2) [21–23] and triboroles (C_2B_3) [24–26] into the regime of well-known anionic *nido*-type carborane clusters (e.g., "dicarbollides") [27–29].

Our group aims to apply dianionic boroles as π-ligands to support electron-rich, low-valent main group atoms. In the past, boroles had already been successfully used in transition metal [30–39] and s-block element coordination [32, 40–43]. Compared to ionic alkali metal salts and highly efficient covalent transition metal bonding, the p-block elements form expectably weaker covalent interactions with the borole π-system. One key obstacle for the successful extension of the dianionic borole ligand into p-block

This is an open access article under the terms of the Creative Commons Attribution License, which permits use, distribution and reproduction in any medium, provided the original work is properly cited.
© 2026 The Author(s). *Angewandte Chemie International Edition* published by Wiley-VCH GmbH

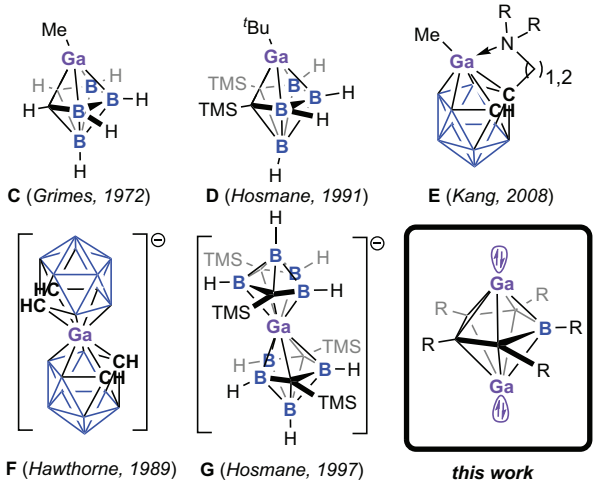

SCHEME 1 | Selected previously structurally authenticated gallacarborane clusters. Blue edges in cluster polyhedra represent BH sites.

chemistry is its propensity to react as a reducing agent toward p-block precursors rather than a metathetic source of the ligand [44–46]. Only recently successful strategies were developed to allow for isolation of divalent group 14 element E(+II) (E = Si, Ge, Sn) compounds of boroles [46–49]. We would now like to report on the successful synthesis and chemistry of two boroledііde ligands (**A** and **B**) supporting two mono-valent Ga(I) centers in a pentagonal-bipyramidal "inverse sandwich" compound, or 1,7-Digallatetra-carborane. Previously known gallacarborane-clusters are limited to Ga(+III) compounds (selected examples **C**–**G**, Scheme 1) [50–54]. 1,7-digallatetracarborane thus represents a significant extension of this chemical space and reveals broad and unique reactivity.

2 | Results and Discussion

When a solution of the toluene solvate of the dilithio derivative of borole **A**, **A**[(Li(tol)]$_2$ in toluene was treated with an excess of Cp*Ga, clean formation of a new compound **1** was observed over the course of three days (Scheme 2). Compound **1** could be isolated in good yields of 84% as a colorless solid and identified to be the *closo*-1,7-digallatetracarborane cluster or the "inverse" sandwich compound of a borole dianion and two Ga(I) atoms capping both sides of the central five-membered heterocycle. The

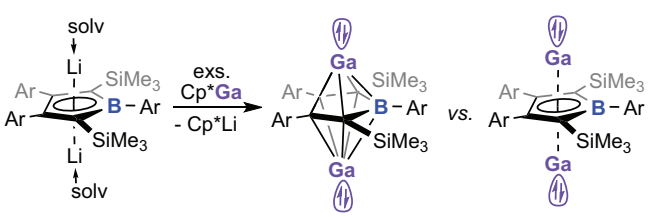

SCHEME 2 | Synthesis of Ga(I) "inverse" borole sandwich compounds **1** and **2** and its alternative depiction as *closo*-digallacarborane clusters.

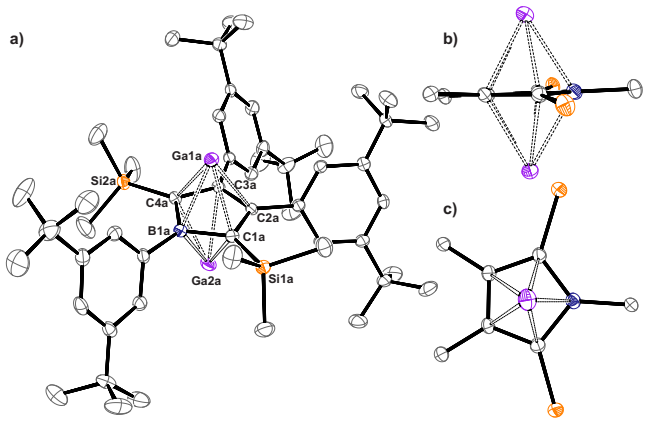

FIGURE 1 | Perspectives on the molecular structure of *closo*-digallacarborane **2**. Atomic displacement parameters shown at 50% probability. A second molecule in the asymmetric unit, hydrogen atoms, as well as minor disorder of organic moieties, are not shown for the sake of clarity. Selected bond lengths [Å] and angles [°] are: B1a–C1a 1.559(3), C1a–C2a 1.455(3), C2a–C3a 1.439(3), C3a–C4a 1.459(3); B1a–C4a 1.551(3), B1a–Ga1a 2.399(3), C1a–Ga1a 2.412(3), C2a–Ga1a 2.438(2), C3a–Ga1a 2.422(2), C4a–Ga1a 2.413(3), B1a–Ga2a 2.410(3), C1a–Ga2a 2.437(3), C2a–Ga2a 2.440(2), C3a–Ga2a 2.460(3), C4a–Ga2a 2.435(3). Ctr_{BC4}–Ga1a 2.056, Ctr_{BC4}–Ga2a 2.079, Ga1a–Ctr_{BC4}–Ga2a 175.97°.

proposed constitution of **1** is corroborated by mass spectrometry, NMR-spectroscopy, elemental analysis, and (most convincingly) by subsequent reactivity studies (*vide infra*), but could not be unambiguously proven by X-ray crystallography as we remained unable to obtain suitable single crystals.

However, we also performed respective lithium–gallium metathesis reactions with the dilithio compound of a related borole substitution derivative **B**[Li(Et$_2$O)]$_2$ and successfully obtained the analogous digallium compound **2** in combined yields of 53%. Single crystals suitable for X-ray diffraction of **2** were obtained and unambiguously reveal the proposed structure of the pentagonal bipyramid (Figure 1). We have no reason to assume a deviating structural motif for **1**. Monitoring the formation of **1** and **2** via NMR spectroscopy suggests a reasonable stepwise exchange of Li^+ against Ga^+ via a heterobimetallic mixed Li^+/Ga^+ intermediate. At the beginning, ^{7}Li NMR spectroscopy reveals the rather highfield-shifted resonance of **A**(Li)$_2$ with $\delta(^7Li) = -8.9$ ppm (**A**[Li(tol)]$_2$/−6.0 (**A**[Li(Et$_2$O)]$_2$). In the course of the reaction, an intermediate featuring a further ^{7}Li resonance (shifted to higher frequencies around $\delta(^7Li) = -3$ ppm) along with a further set of ^{1}H resonances characteristic for a borole containing species can be observed. We propose this intermediate to be the putative mixed Li^+/Ga^+ intermediate (see Figure SI4) [55]. We have tried to independently access and isolate this intermediate from reactions of **A**/**B**(Li$_2$) with one equiv. of Cp*Ga and can confirm predominant formation of the respective Li^+/Ga^+ intermediate, but failed sofar to obtain pure material that would allow unambiguous characterization.

It is important to note that the solvation of the dilithio boroldiide starting material is crucial for the successful full conversion and itself depends on the substitution pattern of the borole. While the ether adduct **B**[Li(Et$_2$O)]$_2$ can be applied to slowly but reliably produce **2**, the presence of any amount of residual ether will

15213773, 2026, 33, Downloaded from https://onlinelibrary.wiley.com/doi/10.1002/anie.6667904 by Universitatsbibliothek RWTH Aachen University, Wiley Online Library on [29/10/2026]. See the Terms and Conditions (https://onlinelibrary.wiley.com/terms-and-conditions) on Wiley Online Library for rules of use; OA articles are governed by the applicable Creative Commons License

suppress the successful full conversion and isolation of **1** from **A**$(Li)_2$. For this reason, we specifically targeted to access the toluene solvate **A**$[Li(tol)]_2$.

In our hands, the amount of ether donor present in the starting material, ranging from one down to approximately 0.2 ether molecules per lithium atom, simply depending on how excessively **A**$[Li(Et_2O)_n]_2$ was dried in vacuo, significantly influenced the conversion times to **2**. The clear relationship is that the lower the ether content, the faster the conversion. We reason that increasing amounts of ether liberated during the course of the reaction stabilize the lithium–boroldiide interaction and progressively hamper efficient substitution of Li^+ against Ga^+.

The molecular structure of **2** features two Ga(I) atoms occupying the apical positions of a pentagonal bipyramid, with both Ga atoms sitting centrally over the $[BC_4]$-cycle as indicated by the Ga-Ctr_{BC4}-Ga angle of approximately 176°. Ga1a sits slightly closer to the central borole moiety (Ctr_{BC4}–Ga1a 2.056 Å) than Ga2a (2.079 Å). The bond lengths of the central $[C_4B]$-moiety (B–C_α 1.55 Å, C_α–C_β 1.46 Å, and C_β–C_β 1.44 Å; where $C_\alpha = C_{1,4}$ and $C_\beta = C_{2,3}$ of the borole C_4B) are very similar to those in the parent dilithio boroledиide **A**$[Li(tol)]_2$ (B–C_α 1.54 Å, C_α–C_β 1.46 Å, and C_β–C_β 1.43 Å; Figure SI1) indicating preservation of the boroledиide moiety upon coordination of Ga(I).

NMR spectroscopic characteristics of **1** (**2**) reveal resonances at $\delta(^{11}B)$ = 31.5 (32.4) ppm, roughly in the range of basal B-atoms in known *closo*-carboranes [52]. $^{13}C_\alpha$ and $^{13}C_\beta$ resonate at 132.5 (132.7) and 145.5 (143.6) ppm, respectively. ^{11}B- and ^{13}C-NMR shifts can be compared to previously reported low-valent main-group borole compounds [48, 49]. ^{13}C-resonances (particularly C_α) reveal substantial low-field shifts (e.g., compared to the parent dilithio compound **A**$(Li)_2$ [C_α 104.6; C_β 128.5 ppm]). Attempts to detect ^{71}Ga-NMR resonances failed for **1** and **2,** likely due to unsuitable correlation times leading to signal broadening beyond recognizability, even at elevated temperatures [56]. This is fully in line with previous ^{71}Ga-NMR studies conducted on bulky Cp^RGa derivatives by Schnöckel and coworkers [57]. A number of neutral *closo* (**C**, **D**, **E**) and anionic *commo*-galla(di)carborane (**F**, **G**) clusters (Scheme 1) have been previously prepared and structurally characterized; however, all of these are richer in boron and exclusively feature Ga(III) atoms [50–54]. In *ortho*-(di)carbollide-type ligand systems **C**–**F**, the Ga atom sits slightly dislocated from the center of the five-membered coordination face, maximizing short contacts to more polarizable boron atoms [27].

This acentric location of the Ga atom in Ga(III) triboroldiide compounds **C**–**F** hints at a more evenly distributed charge density in boroledиide compounds discussed here. As to be expected for larger ionic radii, the Ga(I) atoms in **2** reveal longer contacts to the boroledиide (Ctr_{BC4}–Ga 2.05–2.08) ligand compared to all cases of the Ga(III) atoms in **C**–**F** which sit much closer to the dianionic $[C_2B_3]$-ligand (Ga–Ctr_{B3C2} approximately 1.78–1.93 Å).

Compound **1** revealed thermal stability in solution up to 80°C for several days without any sign of decomposition.

Within the small series of known, loosely related compounds, *closo*-1,7-digallatetracarborane clusters **1** and **2** uniquely feature nucleophilic Ga(I) atoms with lone-pairs of electrons that can engage in further chemistry of the cluster. Recently, digallylenes featuring two flexibly bridged Ga(I) ions in spatial proximity have been shown to reveal cooperative reactivity [58–62].

The cation $[GaCp^*Ga]^+$, previously reported by Fischer and coworkers and later by Schorpp and Krossing, is iso-electronically related to **1** and **2** [63, 64]. The Ga–Ctr_{Cp^*} (2.228 and 2.237 Å) in this cation is considerably longer than in **2**, in line with increased electrostatic interactions of Ga^+ with the dianionic ligand. Accordingly, the nature of $[GaCp^*Ga]^+$ was described to feature a rather weak and readily dissociating arene–Ga^+ interaction between the neutral GaCp* molecule and a Ga(I) ion. Thus, $[GaCp^*Ga]^+$ reacts as a source of Ga^+ and GaCp* individually, rather than as an authentic stable *closo*-cluster or an "inverse sandwich" compound [63, 65]. EDA analysis for the bonding interactions between $[Ga(H_4C_4BH)]^-$ and GaCp* with a Ga^+ ion allows direct comparison between **H** and $[GaCp^*Ga]^+$.

Next to obviously higher electrostatic interactions in **H**, the ΔE_{orb} value describing covalent interaction is significantly higher in **H** (−97.5 kcal mol^{-1}) than in $[GaCp^*Ga]^+$ (−75.5 kcal mol^{-1}) (see Table SI3). To gain further insight into the bonding in such *closo*-1,7-digallatetracarborane clusters, DFT (BP86-D3BJ/def2-TZVP) calculations were performed on **1**/**2** as well as on the parent model compound $Ga(H_4C_4BH)Ga$ **H** and a summary on the frontier molecular orbitals of **H** is depicted in Figure 2 [66–72]. The MO pattern observed in **H** is representative for **1** and **2**, for which corresponding motifs were identified in respective energetic order (Figures SI23 and SI24).

The HOMO (−5.28 eV) for (H) resides between the two Ga-atom and the $C_\alpha BC_\alpha$-moiety of the borole and reveals strong contributions from both Ga atoms with significant lobes pointing outside the cluster. The HOMO-1 (−6.46 eV) is similar in nature with σ-type interactions of the Ga p-orbitals and the $C_\beta C_\beta$-moiety; however, it is energetically significantly lower and close in energy to HOMO-2 (−6.55 eV). HOMO-2 represents classic π-bonding interactions of each Ga-atom with the π-system of the free boroledиide ligand. However, the contribution of Ga-atom orbitals to HOMO-2 of (H) seems to be small. LUMO and LUMO+1 are essentially linear combinations of empty p-orbitals at Ga-atoms with little to no contribution from the C_4B-moiety. It is noteworthy that the energetic order of the HOMO levels of comparable interactions in isoelectronic $[GaCp^*Ga]^+$ and related Cp*Ga deviates significantly with the latter revealing the Ga–Cp* π-bonding interactions being the HOMO/HOMO-1 and the σ-type interactions being more stable (HOMO-2, Figures SI21 and 22). As expected for η^5-π-complexes, intrinsic bonding orbital analysis reveals delocalized bonding involving two 5c2e-bonds ($Ga_2BC_\alpha C_\beta$) and one 4c2e-bond ($Ga_2C_\beta C_\beta$) as well as two low-lying Ga 4s-orbital based lone pairs (Figure SI27). The HOMO of **1**/**2** is found at −4.87 eV. This points at a potential nucleophilic behavior of these Ga-atoms as the respective HOMO in a comparable Si(II)-borole compound had been calculated at −5.23 eV [48].

To probe the chemical accessibility of the lone pairs of electrons at the Ga(I) atoms, **1** was added to THF solutions of freshly generated tungsten pentacarbonyl complex (thf)$W(CO)_5$. Depending on the applied equivalents of **1** to (thf)$W(CO)_5$ we were able

15213773, 2026, 33, Downloaded from https://onlinelibrary.wiley.com/doi/10.1002/anie.6667904 by Universitatsbibliothek RWTH Aachen University, Wiley Online Library on [29/10/2026]. See the Terms and Conditions (https://onlinelibrary.wiley.com/terms-and-conditions) on Wiley Online Library for rules of use; OA articles are governed by the applicable Creative Commons License

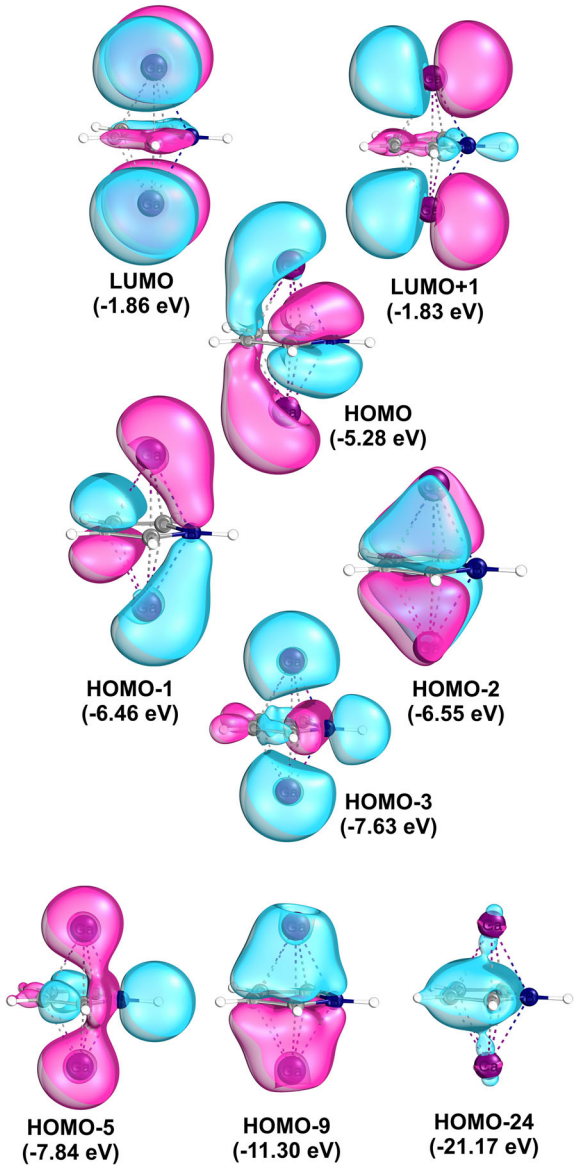

FIGURE 2 | Frontier MO depictions and energies of the parent $Ga(H_4C_4BH)Ga$ (H) (BP86-D3BJ/def2-TZVP). *Iso*-density surfaces are drawn at the 80% level.

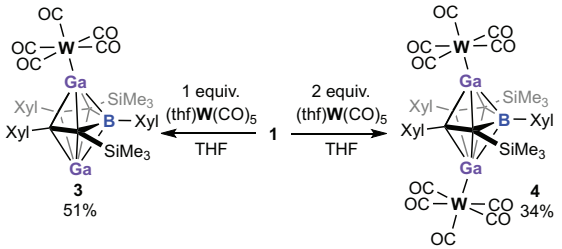

SCHEME 3 | Mono- and bis-adduct formation of **1** with $[(thf)W(CO)_5]$.

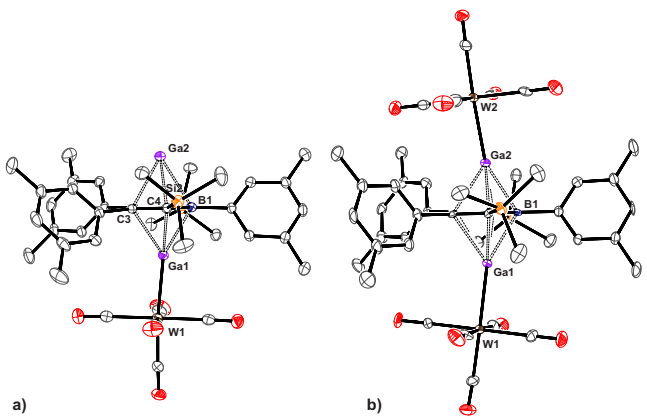

FIGURE 3 | ORTEP depictions of the molecular structures of compounds **3** (a) and **4** (b). Atomic displacement parameters shown at 50% probability. Selected bond lengths [Å] and angles [°] are given. For **3**: B1–Ga2 2.403(2), C1–Ga2 2.444(2), C4–Ga2 2.435(2), C2–Ga2 2.473(2), C3–Ga2 2.446(2), B1–Ga1 2.247(2), C1–Ga1 2.261(2), C4–Ga1 2.291(2), C2–Ga1 2.371(2), C3–Ga1 2.358(2), Ga1–W1 2.5533(5), W1–C_{ax} 1.994(2), W1–C_{eq} 2.038(2)–2.048(2), Ctr_{BC4}–Ga1 1.919, Ctr_{BC4}–Ga2 2.078, Ga1-Ctr_{BC4}-Ga2 172.4°, W1–Ga1–Ga2 173.06(1)°; for **4**: B1–Ga1 2.260(9), B1–Ga2 2.241(9), Ga1–W1 2.547(1), Ga2–W2 2.534(1), W1–C_{ax} 2.003(9), W1–C_{eq} 2.015(9)-2.04(1), W2–C_{ax} 2.002(9), W2–C_{eq} 2.03(1)-2.05(1), Ctr_{BC4}–Ga1 1.934, Ctr_{BC4}–Ga2 1.919, Ga1–Ctr_{BC4}–Ga2 169.6°, W1–Ga1–Ga2 172.47(5)°, W2–Ga2–Ga1 170.18(4)°.

to isolate either the mono-adduct **3** (**1**$[W(CO)_5]$) or the bis-adduct **4** (Scheme 3) as colorless solids in mediocre yields. The molecular structure of both compounds was confirmed by X-ray diffraction (Figure 3), highlighting the potential of **1** to act as a Janus-type ligand in coordination chemistry. Spectroscopically, the first adduct formation barely affects the NMR chemical shifts of potentially indicative nuclei of the starting material, and only the second adduct reveals a minor shift in the ^{11}B resonance.

The ^{11}B NMR signals are found at $\delta(^{11}B)$ = 31.5 (**1**), 31.2 (**3**), and 27.2 (**4**) ppm. The characteristic CO-stretching frequencies of the $[W(CO)_5]$ fragment are observed by ATR-IR spectroscopy of solid samples at 2060/1977/1913 cm^{-1} (**3**) and 2065/1999/1916 cm^{-1} (**4**) indicating a very subtle blue-shift upon addition of the second fragment in line with a decreasing σ-donor strength. Albeit a weak effect, this points to the electronic dependency of the two Ga(I) atoms. Overall, the observed CO-stretching frequencies are in the same range as previously observed for Cp*Ga–$W(CO)_5$ (2065/1986/1910 cm^{-1}) Cp^{iPr5}Ga–$W(CO)_5$ (2062/1913 cm^{-1}) [73, 74].

Closo-digallacarborane (**1**) is thus a slightly more potent σ-donor than Cp*Ga when coordinating to one $[W(CO)_5]$ fragment but reveals almost identical stretching frequencies in its bis-adduct. Computational assessment (BP86-D3BJ/def2-TZVPP/J CPCM = benzene) of this stepwise adduct formation affords a $\Delta H/\Delta G$ of −21.2/−17.7 kcal mol^{-1} for the first adduct formation (**1** to **3**) and −16.9/−11.7 kcal mol^{-1} for the second adduct formation (**3** to **4**). Thus, both reactions are almost equally exothermic. As the enthalpy of adduct formation is barely affected, the slightly reduced free energy of the second addition is likely associated with strongly reduced degrees of freedom in **4**. The computationally approximated thermodynamics (BP86-D3BJ/def2-TZVPP in benzene) for the consecutive formation of **H-W(CO)$_5$** and **H-[W(CO)$_5$]$_2$** from **H** and $(thf)W(CO)_5$ are $\Delta H/\Delta G$ −12.1/−11.9 kcal mol^{-1} for **H-W(CO)$_5$** and −5.3/−4.0 kcal mol^{-1} for **H-[W(CO)$_5$]$_2$**. The second addition is thus significantly less exothermal than the first addition, in line with a reduced nucleophilicity. The

15213773, 2026, 33, Downloaded from https://onlinelibrary.wiley.com/doi/10.1002/anie.6667904 by Universitatsbibliothek RWTH Aachen University, Wiley Online Library on [29/10/2026]. See the Terms and Conditions (https://onlinelibrary.wiley.com/terms-and-conditions) on Wiley Online Library for rules of use; OA articles are governed by the applicable Creative Commons License

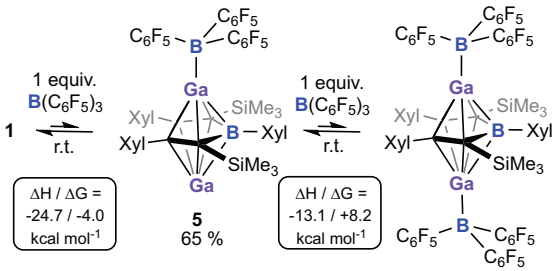

SCHEME 4 | Formation of mono-borane adduct **5**. Thermodynamics at BP86-D3BJ/def2-TZVPP (CPCM = benzene) level of theory at 298 K.

respective MO with a suitable Ga-contribution in **H-W(CO)$_5$** is HOMO-3 found at −6.49 eV in line with significantly reduced Lewis-basicity of the Ga(I) atoms upon adduct formation (see Figure 2).

In **3**, the HOMO is rather delocalized with only a reduced character of a Ga(I) lone-pair of electrons at −5.44 eV, and lower in energy compared to the HOMO of free **1** (−4.87 eV).

The molecular structures of **3** and **4** are depicted in Figure 3. In mono-adduct **3**, the coordinating Ga-atom sits much closer to the ring-plane (Ctr_{BC4}–Ga1 1.92 vs. Ctr_{BC4}–Ga2 2.08 Å) and Ga1 is slightly dislocated toward the C_α-B-C_α-side. The W–C_{ax} distance (1.994(2) Å) is notably shorter than the bonds to the equatorially bound carbonyls indicating a notable *trans*-influence of the gallium(I) donor.

For comparison, the W–CO distances in Cp*GaW(CO)$_5$ are reported at 2.008(5) (C_{ax}) and 2.036(7)–2.059(7) Å for C_{eq}, and the Ga-Ctr_{C5} is found at 1.915 Å [73]. In **4**, both [Ga–W(CO)$_5$] fragments reveal virtually identical bonding features. The Ga–Ga–W angles deviate from linearity for both compounds **3** (173.1°) and **4** (172.5°/170.2°). This structural feature was previously rationalized in Cp*Ga–M(CO)$_5$ (M = Cr, W) by packing effects [73, 75]. For **3**/**4** this deviation from linearity with a bending of the [W(CO)$_5$] fragments away from the B-atom is reasonably in line with the spatial orientation of the Kohn–Sham HOMO (see Figure 2 for representative HOMO of **H**) and thus likely not due to packing. Computationally probed adducts to parent cluster **H-W(CO)$_5$** and **H-[W(CO)$_5$]$_2$** reveal even more pronounced bending (Ga–Ga–W angles of 153° and 156°, respectively).

The ability of Ga(I) atoms in **1** to act as a Lewis-base was also probed against B(C$_6$F$_5$)$_3$ as a well-established main-group Lewis-acid (Scheme 4) [76–80]. The addition of one equiv. of B(C$_6$F$_5$)$_3$ to digalla carborane **1** results in a clear high-field-shift of the ^{19}F-NMR resonance of the *para*-F atom in C$_6$F$_5$ from $\delta(^{19}F)$ = −141.9 ppm to −147.0 ppm, indicative of the formation of a Lewis acid-base adduct **5** [**1**·(B(C$_6$F$_5$)$_3$]. Variable temperature ^{11}B NMR spectroscopy suggests a labile adduct. At ambient temperatures, two overlapping ^{11}B signals are observed at $\delta(^{11}B)$ = 36.5 and 31.8 ppm. Upon cooling, the signal assigned to the bound B(C$_6$F$_5$)$_3$ shifts to lower frequencies (at −50°C, $\delta(^{11}B)$ = −10.2 ppm) into a range expected for such adducts. Borane-adduct **5** can be isolated in good yields of 65% and its structure was corroborated by X-ray diffraction (Figure 4). As observed in tungsten complexes **3**/**4**, the Ga-atom involved in adduct formation (Ga1) sits much

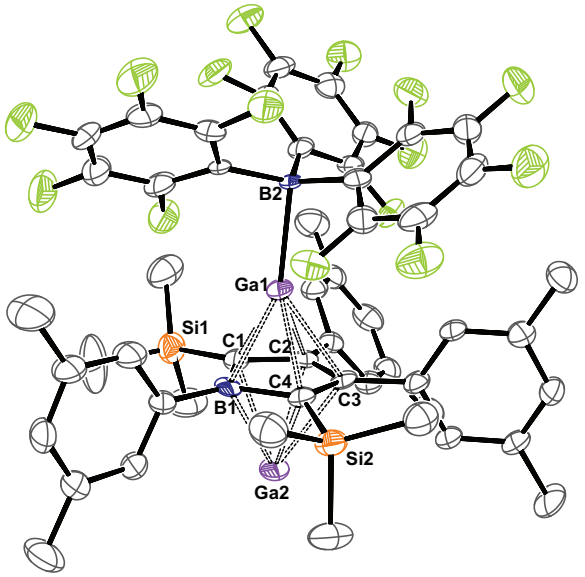

FIGURE 4 | ORTEP depiction of the molecular structure of compound **5**. Hydrogen atoms and lattice pentane molecules are omitted for clarity. Atomic displacement parameters shown at 50% probability. Selected bond lengths [Å] and angles [°] are given. B1–C1 1.568(8), C1–C2 1.488(8), C2–C3 1.437(8), C3–C4 1.470(6), C4–B1 1.581(9), B1–Ga2 2.396(5), C1–Ga2 2.421(5), C2–Ga2 2.432(5), C3–Ga2 2.459(5), C4–Ga2 2.474(5), B1–Ga1 2.245(5), C1–Ga1 2.243(5), C2–Ga1 2.342(5), C3–Ga1 2.359(5), C4–Ga1 2.281(5), Ga1–B2 2.251(5), Ctr_{BC4}–Ga1 1.902, Ctr_{BC4}–Ga2 2.071, Ga1–Ctr_{BC4}–Ga2 172.7°, Ctr_{BC4}–Ga1–B2 170.6°.

closer to the central (C$_4$B) moiety (Ctr_{C4B}–Ga1 1.902 Å; Ctr_{C4B}–Ga2 2.071 Å). Ga2 resides centrally over the (C$_4$B)-ring with small deviations between the individual Ga–(C$_4$B) contacts, similar to those observed in cluster **1**. Ga1 sits slightly dislocated closer to the C_α-B-C_α-side atop the C$_4$B plane, indicated by comparatively long Ga1–C_β contacts.

A number of LGa^{+I} → B(C$_6$F$_5$)$_3$ adducts are documented in the literature, and the Ga–B distances in these are found between 2.108(2) and 2.161(2) Å consistently shorter than in **5** (Ga1–B2 2.251(5) Å) [81–85]. The Ctr_{C5}–Ga contacts in (CpGa) → B(C$_6$F$_5$)$_3$ and (Cp*Ga)→B(C$_6$F$_5$)$_3$ are, however, nearly identical to Ctr_{BC4}–Ga1 [81, 84, 86].

Unlike mono-[W(CO)$_5$] adduct **3**, B(C$_6$F$_5$)$_3$-adduct **5** does not engage in further adduct formation, but instead free B(C$_6$F$_5$)$_3$ is in dynamic exchange with bound borane in mono-adduct **5**. This is corroborated by spectroscopic insight as upon stepwise addition of a further equivalent of borane B(C$_6$F$_5$)$_3$ to solutions of **5**, ^{19}F- NMR-monitoring reveals only a single set of signals for a (C$_6$F$_5$)-moiety.

With increasing borane content, the *ortho*-, *meta*-, and *para*-^{19}F-resonances observed in **5** are increasingly shifted back toward free B(C$_6$F$_5$)$_3$. In mixtures formally containing **1** and two equivalents of B(C$_6$F$_5$)$_3$ the ^{19}F resonances are observed close to the averages between pure **5** and B(C$_6$F$_5$)$_3$.

Computational insight (BP86-D3BJ/def2-TZVPP/J CPCM = benzene) into the thermodynamics (at 298 K) of this reaction is

15213773, 2026, 33, Downloaded from https://onlinelibrary.wiley.com/doi/10.1002/anie.6667904 by Universitatsbibliothek RWTH Aachen University, Wiley Online Library on [29/10/2026]. See the Terms and Conditions (https://onlinelibrary.wiley.com/terms-and-conditions) on Wiley Online Library for rules of use; OA articles are governed by the applicable Creative Commons License

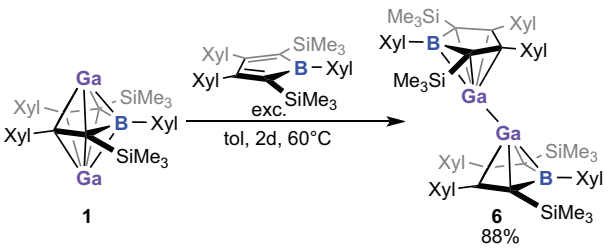

SCHEME 5 | Formation of digallane-type digallocene **6** by two-electron oxidation of *closo*-digallacarborane **1** with free borole **A**.

shown in Scheme 4. Both adduct formations are predicted to be exothermal, but the second adduct reveals a notably reduced ΔH. The second addition is accordingly predicted endergonic (ΔG = +8.2 kcal mol^{-1}) whereas the first addition is still exergonic (ΔG = −4.0 kcal mol^{-1}) fully in line with the experimental observations. The HOMO in **5** strongly resembles the HOMO in **1** and should thus be considered to be involved in further Ga-bonding.

It is energetically predicted at −5.69 eV and thus more stabilized than the HOMO in mono-[W(CO)$_5$]-adduct **3** (−5.44 eV, *vide supra*). The behavior of *closo*-1,7-digalla-tetracarborane **1** toward B(C$_6$F$_5$)$_3$ thus clearly indicates a dependency of the basicity of the two Ga(I) atoms and thus electronic communication between the Ga-atoms within the cluster framework. We further anticipated studying electronic communication by the Ga(I) atoms and conducted cyclovoltammetric (CV) measurements, expecting to observe two distinct consecutive oxidative events for each individual Ga atom. However, in our hands, we failed to obtain meaningful CV data as reproducibly detrimental electrode-fouling occurred with the formation of a metallic layer on the glassy carbon working electrode after a single cycle at both oxidative and reductive potentials. Yet, we succeeded in chemically oxidizing *closo*-1,7-digallatetra-carborane **1** selectively by adding an excessive amount of free borole **A** (1,3,4-Xyl$_3$-2,5-(SiMe$_3$)-borole) to solutions of **1** with full conversion of **1** after two days at 60°C (Scheme 5).

Borole **A** serves as a two-electron oxidant toward **1**, cleanly yielding the unprecedented digallocene **6** in excellent yields of 88% as an orange solid after the removal of excessive borole. An excess of free borole and elevated temperatures were applied, as consumption of **1** and formation of **6** under stoichiometric conditions at room temperature are drastically slowing down in the course of the reaction, and we did not observe complete conversion even after several weeks. Crystals suitable for X-ray analysis were obtained from saturated solutions in toluene and reveal an unusual dimetallocene-type structure (Figure 5). Both Ga(I) atoms in **1** are formally oxidized to Ga(II) and a Ga–Ga bond forms between two **A**(Ga)-fragments. Only very few dimetallocene derivatives Cp^{R}M-MCp^R (M = Be^{+I} [87, 88], Zn^{+I} [89, 90], and Li$^+$/(Al or Ga)$^{+I}$ [74, 91]), are known and still represent synthetically very demanding and intriguing motifs. The latter "dimetallocenes", however, do not constitute covalent M–M bonds but rather feature weak dative M → M' interactions.

The digallane/digallocene compound **6** represents the first dimetallocene-type sandwich compound with an unusual [M$_2$]$^{4+}$ core of low-valent group 13 metals coordinated by the boroledиide,

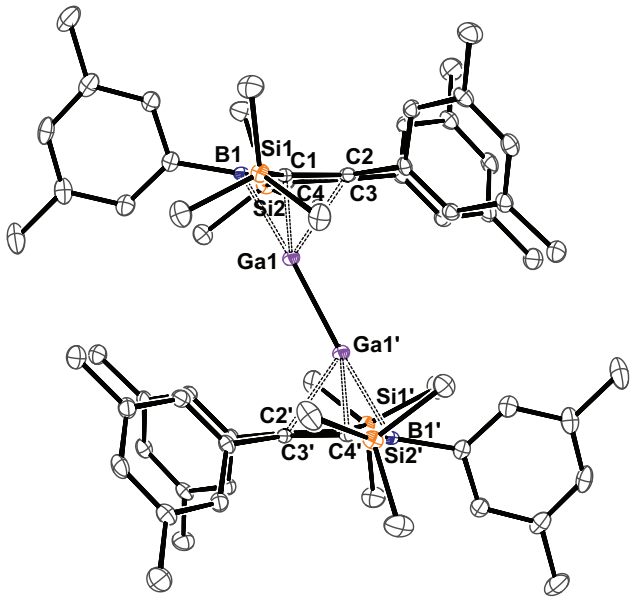

FIGURE 5 | ORTEP depiction of the molecular structure of compound **6**. Hydrogen atoms and a lattice toluene molecule are omitted for clarity. Atomic displacement parameters shown at 50% probability. Selected bond lengths [Å] and angles [°] are given. Ga1–Ga1' 2.3701(4), B1–C1 1.581(2), C1–C2 1.462(1), C2–C3 1.429(2), C3–C4 1.459(1), C4–B1 1.575(2), B1–Ga1 2.162(1), C1–Ga1 2.149(1), C2–Ga1 2.294(1), C3–Ga1 2.292(1), C4–Ga1 2.147(1), Ctr$_{BC4}$–Ga1 1.804, Ctr$_{BC4}$–Ga1–Ga1' 145.2°, B1–Ga1–Ga1' 176.8°.

electronically mimicking the typically applied cyclopentadienyls Cp^R. Moreover, to the best of our knowledge, digallane **6** is the first structurally characterized dimetallocene of any group 13 metal. Known examples of classic Cp-based dimetallocenes with a dicationic [M$_2$]$^{2+}$ moiety reveal essentially perpendicular orientation of the M–M bond with regards to the Cp plane (Ctr$_{CpR}$–M–M ≈ 180°).

However, **6** reveals pronounced deviation of linearity/perpendicularity (Ctr$_{C4B}$–Ga1–Ga1' = 145.2°). This deviation from the linear arrangement of Ctr$_{BC4}$-Ga-Ga is reproduced by computational DFT optimization of the structure. This deviation likely stems from asymmetric charge distribution and shape of the relevant frontier molecular orbitals on the dianionic, C_{2v}-symmetric borole-fragment compared to cyclopentadienide of D_{5h} symmetry. To allow for improved orbital interaction between Ga-atom and the ligand, this results in a preferential tilted orientation of the Ga–Ga vector of the [Ga–Ga]$^{4+}$ fragment toward the [C$_\alpha$BC$_\alpha$] moiety in the boroledиide **A**$^{2-}$ rather than a perpendicular orientation toward the centroid of the heterocycle. It is worthy to note that the preference of a Ga atom to interact stronger with the [C$_\alpha$BC$_\alpha$] moiety increases with the formal oxidation number of Ga. Only naked Ga^{+I} atoms (as in **2**) reveal little spatial preference in their coordination behavior toward [C$_4$B].

The structure of **6** resembles the only comparable digallane reported by Hosmane, Cowley and coworkers. They describe a twofold *nido*-carborate [(BH)$_4$(CSiMe$_3$)$_2$]$^{2-}$ capped [Ga–Ga]$^{4+}$ fragment as a low-yielding side-product obtained from the reaction of Na$_2$[(BH)$_4$(CSiMe$_3$)$_2$] with ^{t}BuGaCl$_2$ (Ctr$_{C2B3}$–Ga–Ga

15213773, 2026, 33, Downloaded from https://onlinelibrary.wiley.com/doi/10.1002/anie.666904 by Universitatsbibliothek RWTH Aachen University, Wiley Online Library on [29/10/2026]. See the Terms and Conditions (https://onlinelibrary.wiley.com/terms-and-conditions) on Wiley Online Library for rules of use; OA articles are governed by the applicable Creative Commons License

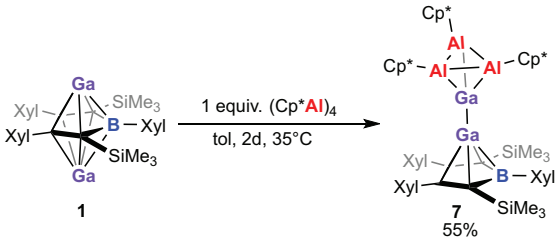

SCHEME 6 | Formation of *conjuncto*-cluster **7** by reaction of *closo*-digallacarborane **1** with $(Cp^*Al)_4$.

= 159.6°/164.4°) [92]. The Ga–Ga distance of **6** (2.3722(4) Å) is slightly longer than reported for Hosmane/Cowley's system (2.340(2) Å) but well in the common range (2.33–2.39 Å) of other digallanes for which diverse coordination environments are known [93–99]. We found neither experimental nor computational indication that could advocate for a putative dimeric hydride $[(borole)Ga^{+III}H]_2$ instead of the digallocene **6** [100].

Given the unique structure of **1**, we also anticipated accessing the putative homologous "inverse sandwich" 1,7-dialuminatetracarborane for which we have so far not found viable synthetic routes. In an attempt to metathetically exchange Ga^{+I} versus Al^{+I}, digallium cluster **1** was treated with $(Cp^*Al)_4$ [7, 9, 101]. Instead of Al/Ga exchange, major rearrangements occur, and the formation of a new, intensely red *conjuncto*-cluster **7** is observed (Scheme 6).

In the presence of excessive AlCp*, the conversion of **1** to **7**, as monitored by NMR-spectroscopy, progresses rather cleanly over the course of two days. The resulting brick-red compound **7** can be isolated in moderate yields of 55%. However, solutions of isolated crystals of **7** reveal partial decomposition to the starting materials until mixtures of stable composition (approximately 0.8 equiv. of **7** vs. 0.2 equiv. of **1**) are obtained after approximately four days, strongly suggesting an equilibrium. This is corroborated by a rather weak exergonicity of the reaction, as predicted by DFT calculations [102].

The molecular structure of **7** was identified by X-ray crystallography (Figure 6). One Ga atom is separated from the digallium cluster and incorporated in a tetrahedral $[GaAl_3]$ cluster fragment, revealing a Ga–Ga interaction with the remaining borole-bound Ga-atom. The Ga1–Ga2 separation (2.5482(8) Å) is significantly longer than in dimetallocene-type digallane **6** (2.3701(4) Å).

An adequate bonding description of **7** is likely best addressed on the grounds of structural features. Two fundamental fragmentations of **7** seem plausible (Scheme 7). It can be seen as a borole-derived gallyl gallylene $\mathbf{A}Ga^{+II}–Ga^{0}$, which replaces one Cp*Al: fragment in the iconic parent tetrameric $(Cp^*Al)_4$ (**7a**, Scheme 7). Alternatively, **7** may be described as a formally monoanionic, Ga-nucleophilic *nido*-cluster $[\mathbf{A}Ga^{+I}]^-$ forming an electrostatically dominated Ga–Ga bond to a Ga-electrophilic $[GaAl_3Cp^*_3]^+$ fragment (**7b**, Scheme 7).

The borole-bound Ga1 atom is located rather centered over the borole ligand, similar to what is otherwise only observed for the coordination mode of Ga^{+I} atoms as in **1** and thus advocates for

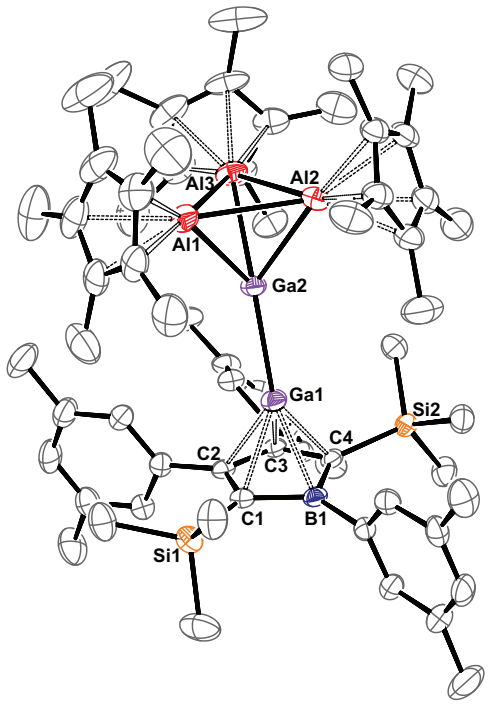

FIGURE 6 | ORTEP depiction of the molecular structure of compound **7**. Hydrogen atoms and a lattice solvent molecule are omitted for clarity. Atomic displacement parameters shown at 50% probability. Selected bond lengths [Å] and angles [°] are given. Ga1–Ga2 2.5482(8), Ga2–Al1 2.554(1), Ga2–Al2 2.545(1), Ga2–Al3 2.577(1), Al1–Al2 2.760(1), Al2–Al3 2.749(1), Al3–Al1 2.764(1), B1–C1 1.553(4), C1–C2 1.451(4), C2–C3 1.429(3), C3–C4 1.455(4), C4–B1 1.549(4), B1–Ga1 2.240(3), C1–Ga1 2.192(2), C2–Ga1 2.254(3), C3–Ga1 2.280(3), C4–Ga1 2.214(3), Ctr_{BC4}–Ga1 1.844, Ctr_{BC4}–Ga1–Ga2 163.3°, B1–Ga1–Ga2 160.5(1)°.

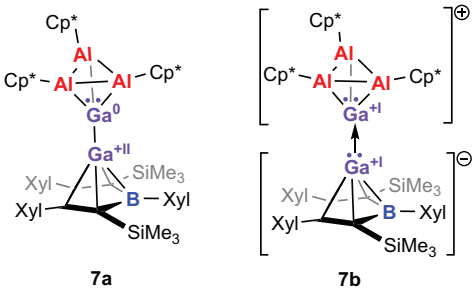

SCHEME 7 | Alternative electronic and bonding descriptions of **A**GaGa$(AlCp^*)_3$ **7**.

the polar description **7b**. The much shorter Ga1–Ctr_{C4B} distance in **7** (1.844 Å) compared to **1** (2.056, 2.079 Å) is explained by the much stronger electrostatic interaction of a borole dianion to a single Ga^+ atom. The electrostatic nature of the Ga–Ga bond in **7b** is further corroborated computationally. NBO analysis finds a polar Ga–Ga bond with 62% contribution of Ga1 (83% s-orbital character, 17% p-orbital character) and 38% from Ga2 (23% s-orbital character, 77% p-orbital character) [103, 104]. Furthermore, an EDA-NOCV analysis of the fragments derived from homolytic versus heterolytic Ga–Ga bond splitting revealed smaller orbital interaction energy values (E_{orb}) for the dative interaction of singlet fragments in **7b**, thus strongly advocating

15213773, 2026, 33, Downloaded from https://onlinelibrary.wiley.com/doi/10.1002/anie.6667904 by Universitatsbibliothek RWTH Aachen University, Wiley Online Library on [29/10/2026]. See the Terms and Conditions (https://onlinelibrary.wiley.com/terms-and-conditions) on Wiley Online Library for rules of use; OA articles are governed by the applicable Creative Commons License

TABLE 1 | Results of an EDA-NOCV calculation to assess the nature of the Ga–Ga bond in **7** (BP86-D3BJ/TZP)[a].

Energy[b]	Homolytic bond scission AGa• •Ga(AlCp*)$_3$ **7**	Heterolytic bond scission [AGa]$^-$ [Ga(AlCp*)$_3$]$^+$
ΔE_{int}	−148.2	−102.5
ΔE_{Pauli}	145.0	126.2
ΔE_{disp}	−28.2	−28.2
ΔE_{elstat}	−91.8	−125.0
ΔE_{orb}	−173.2	−75.5

[a]Performed on the structure obtained from single crystal diffractometry after optimization of H-atoms.
[b]All energies given in kcal mol^{-1}.

for **7b** as the appropriate bonding description [105–108]. The results of the energy decomposition analysis are summarized in Table 1.

The only major contribution to bonding in **7b** according to EDA-NOCV stems from the donation of the *nido*-cluster [**A**Ga^{+I}]$^-$ fragments highest and second highest SFO into the lowest unoccupied SFO of the [Ga(AlCp*)$_3$]$^+$ amounting to 54 kcal mol^{-1} (Figure 7). The difference density plot of this NOCV clearly reveals charge donation into the Ga–Ga bond as well as into the [GaAl$_3$] cluster, also enhancing the bonding between the tetrahedrally arranged cluster atoms.

The isolated cluster cation [Ga(AlCp*)$_3$]$^+$ was only recently described by Dabringhaus and Krossing and obtained from the reaction of arene complexes of Ga$^+$ ([Ga(PhF)$_{2\text{-}3}$]$^+$ [Al(OC(CF$_3$)$_3$)$_4$]$^-$) with (Cp*Al)$_4$ [109, 110]. They found rather weak Ga–Ga interacting dimers of [Ga(AlCp*)$_3$]$^+$ in the solid state and in cold solutions and observed very long Al–Al distances (3.09(4) Å) in these [Ga(AlCp*)$_3$]$^+$ units, suggesting a pronounced character of three individual Al-donors supporting a Ga$^+$ atom rather than a multicenter-bonded [GaAl$_3$]$^+$ cluster. The Al–Al distances in **7** are much shorter (average 2.755(6) Å) virtually identical to those reported by Dabringhaus and Krossing for a chelating Me$_3$TACN (1,4,7-trimethyl-1,4,7-triazacyclononane) donor adduct to [(Me$_3$TACN)Ga(AlCp*)$_3$]$^+$ [109].

Apparently, the electron density provided by a single donor-site ligand like Ga-nucleophilic [**A**Ga]$^-$ into the cluster LUMO of [Ga(AlCp*)$_3$]$^+$ (see Figure 7) is sufficient to enable multi-center metal-bonding within the [GaAl$_3$]-cluster. The ^{27}Al-NMR resonances in **7** are found at $\delta(^{27}Al)$ = −43.4 ppm virtually identical to those reported for isolated [Ga(AlCp*)$_3$]$^+$ (−43.3 ppm) [109]. We observe no spectroscopic indication for dissociation of the ion pair in **7** in solutions at room temperature and expect an intact Ga–Ga bond. ^{1}H-NOESY NMR spectroscopy confirms spatial proximity of the Cp* moieties and the borole.

According to TD-DFT, the red color of **7** observed at λ = 486 nm is in line with HOMO → LUMO+1 excitations and can be attributed to excitations from the Ga–Ga bond into the degenerate set of perpendicular empty p-orbitals at the Al-bound Ga-atom.

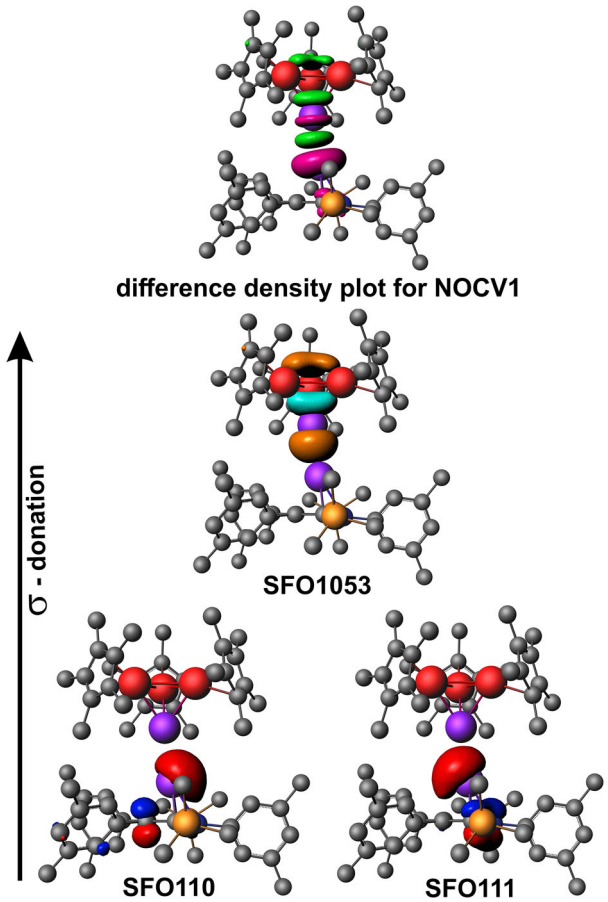

FIGURE 7 | SFO interactions and difference density plot for the NOCV describing the dative Ga–Ga interaction in **7b**. SFO are drawn at an iso-level of 0.05 a.u.; the difference density plot is drawn at 0.003 a.u. blue/red: occupied SFO, orange/turquoise unoccupied SFO, magenta: electron depletion, green: electron accumulation.

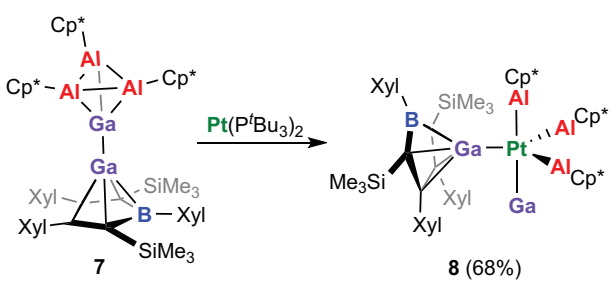

SCHEME 8 | Reaction of **A**GaGa(AlCp*)$_3$ **7** with [Pt(P^{t}Bu$_3$)$_2$] to give complex **8**.

We reason that the formation of **7** occurs by digallium compound **1** reacting as a source of Ga$^+$ ions toward (Cp*Al)$_4$ and thus reveals reactivity rather assignable to an inverse sandwich complex of two individual Ga$^+$ ions than a *closo*-1,7-digallatetracarborane cluster. This is further corroborated by the reactivity of **7** toward [Pt(P^{t}Bu$_3$)$_2$] (Scheme 8). Portion-wise addition of **7** to solutions of [Pt(P^{t}Bu$_3$)$_2$] in toluene over a period of approximately 1 h allows for isolation of platinum complex **8** as a pale yellow-brown powder in yields of 68%. Crystals of **8** suitable for X-ray diffraction were grown from saturated solutions in toluene at −40°C. The molecular structure is shown in Figure 8.

15213773, 2026, 33, Downloaded from https://onlinelibrary.wiley.com/doi/10.1002/anie.666904 by Universitatsbibliothek RWTH Aachen University, Wiley Online Library on [29/10/2026]. See the Terms and Conditions (https://onlinelibrary.wiley.com/terms-and-conditions) on Wiley Online Library for rules of use; OA articles are governed by the applicable Creative Commons License

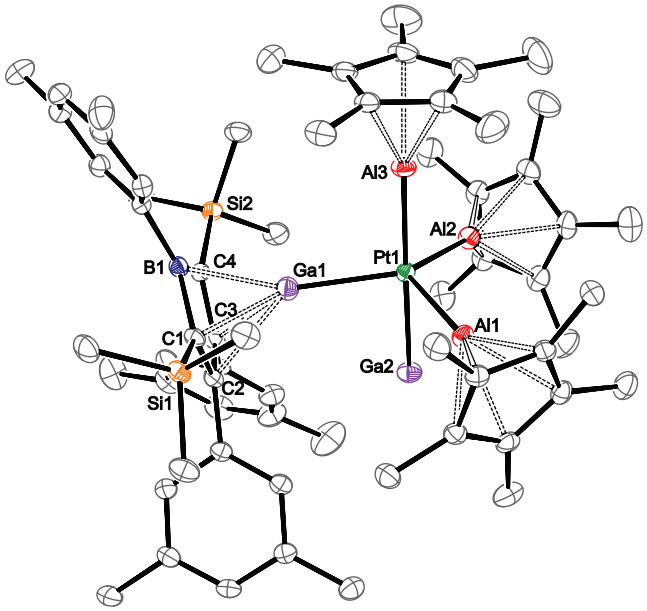

FIGURE 8 | ORTEP depiction of the molecular structure of compound **8**. A second molecule in the asymmetric unit, hydrogen atoms, and co-crystallized toluene molecules are omitted for clarity. Atomic displacement parameters shown at 50% probability. Selected bond lengths [Å] and angles [°] are given. Ga1–Pt1 2.3990(7), Ga2–Pt1 2.4680(6), Al1–Pt1 2.3083(8), Al2–Pt1 2.316(1), Al3–Pt1 2.361(1), B1–C1 1.568(4), C1–C2 1.467(4), C2–C3 1.421(3), C3–C4 1.458(4), C4–B1 1.553(4), B1–Ga1 2.234(3), C1–Ga1 2.231(3), C2–Ga1 2.378(3), C3–Ga1 2.395(3), C4–Ga1 2.225(3), Ctr_{BC4}–Ga1 1.911; Ga1–Pt1–Ga2 83.36(2)°, Ga2–Pt1–Al3 176.13(3)°, Ga1–Pt1–Al1 116.00(3)°, Al1–Pt1–Al2 115.14(4)°, Al2–Pt1–Ga1 124.04°, Ctr_{BC4}–Ga1–Pt1 167.1°.

The platinum atom is inserted into the entire $[Ga(AlCp^*)_3]^+$ cluster with all parts serving as independent ligands, forming a rather unusual penta-coordinate Pt^0-complex with distorted trigonal-bipyramidal coordination geometry. Two (AlCp*) and an isoelec-tronic, yet formally anionic $[\mathbf{A}Ga]^-$ *nido*-cluster occupy the equatorial plane while the axial positions are occupied by a further (AlCp*) and a naked Ga^+ ion. The ligands of the equatorial plane are slightly vaulting over the Ga^+ ligand site with Ga2-Pt-L_{eq} angles between 80° and 85° likely due to repulsion by the sterically more demanding Cp* moiety. The bond lengths within the $[\mathbf{A}Ga]^-$ fragment are similar to those observed in **7** with the only notable difference being the elongated Ga–C_β distances which are approximately 0.1 Å longer.

Cp*E (E = Al, Ga, In) ligands coordinating to zero-valent Ni, Pd, or Pt metal atoms were previously reported by the groups of Jutzi and Fischer [75, 111–117]. Most suitable for comparison, Fischer and coworkers reported the formation of a cationic penta-coordinate $[(Ga)Pt(GaCp^*)_4]^+$ from the reaction of $[Pt(GaCp^*)_4]$ with $[GaCp^*Ga][BAr^F]$, the latter essentially serving as a source of the Ga^+ ligand [65].

Complex **8** thus represents a further, yet neutral, addition to the small number of compounds featuring a naked Ga^+-ligand coordinating to a transition metal [65, 116, 118, 119].

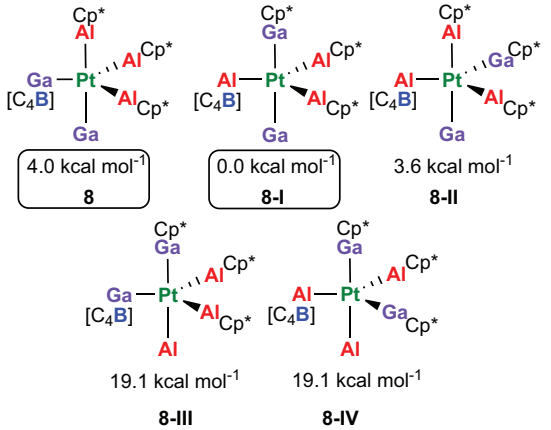

SCHEME 9 | Relative stabilities (ΔG^{298}) of (putative) isomers of complex **8** at r^{2}SCAN-3c (CPCM = benzene) level of theory.

The Pt–$Ga_{terminal}$ distance to the axially located Ga-atom (Pt1–Ga2: 2.4680(6) Å) in **8** is comparable to the one observed by Fischer (2.4593(9) Å), but the equatorially located **A**Ga1–Pt1 distance (2.3990(7) Å) is notably longer than the respective equatorial Pt–(GaCp*) distances (between 2.3474(7) and 2.3577(8) Å) [65]. This can, again, be rationalized by a much more sterically demanding profile of the borole-derived $[\mathbf{A}Ga]^-$ compared to a neutral (Cp*Ga) ligand. We anticipate the bonding situation in **8** to be identical to Fischer's essentially isoelectronic all-Gallium $[(Ga)Pt(GaCp^*)_4]^+$, for which computational assessment suggested the terminal Ga^+ ligand to act as a σ- and π-acceptor ligand to the $[L_4Pt]^0$ fragment [65].

^{1}H-NMR spectroscopy at room-temperature reveals sharp signals for the $[\mathbf{A}Ga]^-$ fragment along with a single, notably broadened signal for the Cp*Al-moiety. This could either indicate structural exchange between equatorially and axially bound AlCp* ligands in solution or even include dynamic Cp* migration from Pt-bound Ga^+ and Al^+ atoms. No signals in ^{71}Ga- and ^{195}Pt-NMR could be detected. No signal is observed in ^{27}Al-NMR spectroscopy (despite precedence for observable signals in chemically related systems) [115]. This further hints at a broadening beyond recognizability by dynamic exchange between AlCp* ligands, Cp* and could potentially even involve exchange of the borole–bound group 13 element. Further experimental hints for such behavior stem from X-ray diffraction. Refinement of the data reveals a slight lack of electron density in the F_o-F_c map at the **A**Ga1 position, suggesting a potential occupation of this site by an Al atom, whereas the axial AlCp* moiety may be partially occupied by GaCp* (Figure SI20). The extent of this potential positional disorder varied slightly between a number of (mediocre) data sets obtained for this compound in the course of our investigations. Scheme 9 summarizes relative stabilities (r^{2}SCAN-3c level of theory) of putative isomers of **8** with regard to Al versus Ga exchange.

Next to the obviously dominating product **8**, isomer **8-I** represents the isomer reasonably associated with the observed residual/lacking electron density in X-ray refinements of **8**. Isomer **8-I** has both axial sites occupied by Ga-atoms and is the most stable isomer within this series of putative compounds (**8** to **8-IV**) according to DFT. While Al-atoms seem to be preferred in equatorial positions and slightly preferred on the borole

15213773, 2026, 33, Downloaded from https://onlinelibrary.wiley.com/doi/10.1002/anie.6667904 by Universitatsbibliothek RWTH Aachen University, Wiley Online Library on [29/10/2026]. See the Terms and Conditions (https://onlinelibrary.wiley.com/terms-and-conditions) on Wiley Online Library for rules of use; OA articles are governed by the applicable Creative Commons License

π-platform, the Al^+-atom as a terminal ligand is energetically clearly disfavored.

It is worth mentioning that such isomers of **8** with regard to the individual occupation of sites between Al and Ga may either result from dynamic exchange in **8**, or result from minor contributions of isomers of the starting material **7**, as Dabringhaus and Krossing already reported on isomerization (i.e., Cp* migration) in $[GaAl_3Cp^*_3]^+$ [109]. Throughout our studies, we have not gathered any further spectroscopic evidence of any of the putative isomers **8-I** to **8-IV**.

3 | Conclusion

We have successfully prepared the first complex of a borole dianion coordinating to two low-valent Ga^+ atoms. This unprecedented *closo*-1,7-digalla-tetracarborane cluster was shown to reveal a rich multifacetted chemistry between a molecular Wade-type cluster and an "inverse" sandwich complex of individually chemically active Ga^+ atoms. Depending on the reagents and reaction conditions, both Ga(I) ions of the digallylene cluster can individually but not independently serve as nucleophilic sites toward tungsten carbonyl fragments rendering **1** a Janus-type metal atom-based ligand. It was shown that the individual basicity of the second Ga-atom is affected upon involvement of the first Ga-atom in Lewis-acid base reactions, thus proving a certain degree of electronic communication between the Ga-sites. The *closo*-1,7-digalla-tetracarborane can be selectively oxidized with free borole to give an unprecedented dimetallocene of the group 13 elements. Toward $(Cp^*Al)_4$, *closo*-1,7-digalla-tetracarborane serves as a Ga^+ donating agent, resulting in an ion pair of an anionic *nido*-1-galla-tetracarborate cluster, which is isoelectronic to iconic neutral Cp*E, and the recently described $[GaAl_3Cp_3^*]^+$ cation. This latter compound was then found to form an intriguing penta-coordinate complex with Pt^0 with a rare terminal Ga^+ ligand further stabilized by Cp*Al and *nido*-1-galla-tetracarborate ligands.

Author Contributions

Julijan Sarcevic: investigation, validation, writing – review and editing, formal analysis, data curation. **Tobias Heitkemper**: investigation, validation, writing – review and editing, formal analysis, data curation. **Niklas Mehner**: investigation, validation, formal analysis, data curation. **Maximilian Kubis**: investigation. **Christian P. Sindlinger**: conceptualization, investigation, validation, data curation, supervision, project administration, funding acquisition, writing – original draft, writing – review and editing, resources.

Acknowledgments

Dedicated to the memory of Prof. Dr. h.c. mult. Herbert W. Roesky. Funded by the Deutsche Forschungsgemeinschaft (DFG, German Research Foundation)—Project number(s) 496024290 (SI2721/2-1) and 538820448 (INST41/1232-1 FUGG). Further co-funding by the European Commission (EFRE Programme BW 2021–2027) is greatly acknowledged. The authors acknowledge support by the state of Baden-Württemberg through bwHPC and the German Research Foundation (DFG) through grant no. INST 40/575-1 FUGG (JUSTUS 2 cluster). We are grateful for the support and provision of research facilities by colleagues, past and present, of the Institutes of Inorganic Chemistry at the University of Göttingen, the RWTH Aachen University, and the University of Stuttgart.

Open access funding enabled and organized by Projekt DEAL.

Conflicts of Interest

The authors declare no conflicts of interest.

Data Availability Statement

Data are provided with this manuscript as Supporting Information. Crystallographic information is provided in the CSD database. Further data can be provided by the authors upon request.

References

1. E. O. Fischer and H. Grubert, "Über Aromatenkomplexe von Metallen. IV. Di-Cyclopentadienyl-Blei," *Zeitschrift für anorganische und allgemeine Chemie* 286 (1956): 237–242, https://doi.org/10.1002/zaac.19562860507.

2. E. O. Fischer and H. Grubert, "Di-Cyclopentadienyl-Zinn," Zeitschrift für Naturforschung. Teil B 11b (1956): 423–424.

3. E. O. Fischer and H. P. Hofmann, "Metall-Cyclopentadienyle des Indiums," *Angewandte Chemie* 69 (1957): 639–640, https://doi.org/10.1002/ange.19570692008.

4. P. Jutzi, F. Kohl, and C. Krüger, "Synthesis and Structure of the Nido-Cluster $(CH_3)_5$ C_5 Sn^+," *Angewandte Chemie International Edition* 18 (1979): 59–60, https://doi.org/10.1002/anie.197900591.

5. P. Jutzi, F. Kohl, P. Hofmann, C. Krüger, and Y.-H. Tsay, "Bis(pentamethylcyclopentadienyl)germanium und -zinn sowie (Pentamethylcyclopentadienyl)germanium- und -zinn-Kationen: Synthese, Struktur und Bindungsverhältnisse," *Chemische Berichte* 113 (1980): 757–769, https://doi.org/10.1002/cber.19801130233.

6. P. Jutzi, D. Kanne, and C. Krüger, "Decamethylsilicocene—Synthesis and Structure," *Angewandte Chemie International Edition* 25 (1986): 164–164, https://doi.org/10.1002/anie.198601641.

7. C. Dohmeier, C. Robl, M. Tacke, and H. Schnöckel, "The Tetrameric Aluminum(I) Compound $[\{Al(\eta^5\text{-}C_5Me_5)\}_4]$," *Angewandte Chemie International Edition* 30 (1991): 564–565, https://doi.org/10.1002/anie.199105641.

8. D. Loos, H. Schnöckel, J. Gauss, and U. Schneider, "$[Ga(C_5H_5)]$: Synthesis, Identification, and Ab Initio Investigations," *Angewandte Chemie International Edition* 31 (1992): 1362–1364, https://doi.org/10.1002/anie.199213621.

9. S. Schulz, H. W. Roesky, H. J. Koch, G. M. Sheldrick, D. Stalke, and A. Kuhn, "A Simple Synthesis of $[(Cp^*Al)_4]$ and Its Conversion to the Heterocubanes $[(Cp^*AlSe)_4]$ and $[(Cp^*AlTe)_4]$ ($Cp^* = \eta^5\text{-}C_5(CH_3)_5$)," *Angewandte Chemie International Edition* 32 (1993): 1729–1731, https://doi.org/10.1002/anie.199317291.

10. D. Loos, E. Baum, A. Ecker, H. Schnöckel, and A. J. Downs, "Hexameric Aggregates in Crystalline (Pentamethylcyclopentadienyl)Gallium(I) at 200 K," *Angewandte Chemie International Edition* 36 (1997): 860–862, https://doi.org/10.1002/anie.199708601.

11. P. Jutzi, A. Mix, B. Rummel, W. W. Schoeller, B. Neumann, and H.-G. Stammler, "The $(Me_5C_5)Si^+$ Cation: A Stable Derivative of HSi^+," *Science* 305 (2004): 849–851, https://doi.org/10.1126/science.1099879.

12. P. Jutzi and N. Burford, "Structurally Diverse π-Cyclopentadienyl Complexes of the Main Group Elements," *Chemical Reviews* 99 (1999): 969–990, https://doi.org/10.1021/cr941099t.

13. G. Linti and H. Schnöckel, "Low Valent Aluminum and Gallium Compounds—Structural Variety and Coordination Modes to Transition Metal Fragments," *Coordination Chemistry Reviews* 206–207 (2000): 285–319, https://doi.org/10.1016/S0010-8545(00)00339-8.

14. S. González-Gallardo, T. Bollermann, R. A. Fischer, and R. Murugavel, "Cyclopentadiene Based Low-Valent Group 13 Metal Compounds:

15213773, 2026, 33, Downloaded from https://onlinelibrary.wiley.com/doi/10.1002/anie.6667904 by Universitatsbibliothek RWTH Aachen University, Wiley Online Library on [29/10/2026]. See the Terms and Conditions (https://onlinelibrary.wiley.com/terms-and-conditions) on Wiley Online Library for rules of use; OA articles are governed by the applicable Creative Commons License

Ligands in Coordination Chemistry and Link Between Metal Rich Molecules and Intermetallic Materials," *Chemical Reviews* 112 (2012): 3136–3170, https://doi.org/10.1021/cr2001146.

15. M. Saito and M. Yoshioka, "The Anions and Dianions of Group 14 Metalloles," *Coordination Chemistry Reviews* 249 (2005): 765–780, https://doi.org/10.1016/j.ccr.2004.08.004.

16. V. Y. Lee and A. Sekiguchi, "Aromaticity of Group 14 Organometallics: Experimental Aspects," *Angewandte Chemie International Edition* 46 (2007): 6596–6620, https://doi.org/10.1002/anie.200604869.

17. X. Sun and P. W. Roesky, "Group 14 Metallole Dianions as η^5-Coordinating Ligands," *Inorganic Chemistry Frontiers* 10 (2023): 5509–5516, https://doi.org/10.1039/D3QI01342A.

18. B. Goldfuss and P. V. R. Schleyer, "Aromaticity in Group 14 Metalloles: Structural, Energetic, and Magnetic Criteria," *Organometallics* 16 (1997): 1543–1552, https://doi.org/10.1021/om960994v.

19. W. P. Freeman, T. D. Tilley, A. L. Rheingold, and R. L. Ostrander, "A Stable η^5-Germacyclopentadienyl Complex: [($\eta^5C_5Me_5$)Ru{η^5-$C_4Me_4GeSi(SiMe_3)_3$}]," *Angewandte Chemie International Edition* 32 (1993): 1744–1745, https://doi.org/10.1002/anie.199317441.

20. W. P. Freeman, T. D. Tilley, and A. L. Rheingold, "Stable Silacyclopentadienyl Complexes of Ruthenium: (η^5-C_5Me_5)Ru[η^5-$Me_4C_4SiSi(SiMe_3)_3$] and X-Ray Structure of Its Protonated Form," *Journal of the American Chemical Society* 116 (1994): 8428–8429, https://doi.org/10.1021/ja00097a085.

21. D. Scheschkewitz, M. Menzel, M. Hofmann, et al., "A Five-Membered Ring With Three Negative Charges and Solvent-Free Lithium Counterions," *Angewandte Chemie International Edition* 38 (1999): 2936–2939, https://doi.org/10.1002/(SICI)1521-3773(19991004)38:19%3c2936::AID-ANIE2936%3e3.0.CO;2-9.

22. H. Wadepohl, H. Pritzkow, and W. Siebert, "Bis[Cyclopentadienyl(1,3-Diborolenyl)Cobalt]tin. A Stannocene Analog With a Bent Tetradecker Sandwich Structure," *Organometallics* 2 (1983): 1899–1901, https://doi.org/10.1021/om50006a042.

23. K. Stumpf, H. Prizkow, and W. Siebert, "Synthese und Struktur eines Thalliumkomplexes mit anionischem Sandwichkomplex als Ligand," *Angewandte Chemie* 97 (1985): 64–65, https://doi.org/10.1002/ange.19850970121.

24. M. Unverzagt, H.-J. Winkler, M. Brock, et al., "Reduction of Dicarbapentaboranes(5) to 1,2-Diborata-4-Boracyclopentadienes: Antiaromatic Compounds With 4π-Electron Systems," *Angewandte Chemie International Edition* 36 (1997): 853–855, https://doi.org/10.1002/anie.199708531.

25. W. T. Robinson and R. N. Grimes, "Crystal and Molecular Structure of 2-methyl-1,7-bis(η^5-cyclopentadienyl)-1,7,2,4-Dicobaltadicarbaheptaborane(7), a Triple-Decked Sandwich Compound," *Inorganic Chemistry* 14 (1975): 3056–3059, https://doi.org/10.1021/ic50154a040.

26. X. Wang, M. Sabat, and R. N. Grimes, "Organotransition-Metal Metallacarboranes. 43. Directed Synthesis of Carborane-End-Capped Multidecker Sandwiches," *Journal of the American Chemical Society* 117 (1995): 12227–12234, https://doi.org/10.1021/ja00154a024.

27. N. S. Hosmane and J. A. Maguire, "Syntheses, Structures, Bonding, and Reactivity of Main Group Heterocarboranes," in Advances in Organometallic Chemistry, *Volume 30*, ed. F. G. A. Stone and R. West (Academic Press, 1990), 99–150.

28. A. H. Cowley, P. Galow, N. S. Hosmane, P. Jutzi, and N. C. Norman, "The Structures of Seven-and Twelve-vertex Stannacarbaboranes and Their Relationship to Cyclopentadienyl Tin Cations," *Journal of the Chemical Society, Chemical Communications* (1984): 1564, https://doi.org/10.1039/c39840001564.

29. N. S. Hosmane, K. J. Lu, H. Zhang, A. H. Cowley, and M. A. Mardones, "Synthesis and Crystal Structure of a Closo-Indacarborane Dimer," *Organometallics* 10 (1991): 392–393, https://doi.org/10.1021/om00048a011.

30. G. E. Herberich, J. Hengesbach, U. Kölle, G. Huttner, and A. Frank, "A Novel Type of Triple-Decker Complex—Borole as Bridging Ligand," *Angewandte Chemie International Edition* 15 (1976): 433–434, https://doi.org/10.1002/anie.197604332.

31. G. E. Herberich, J. Hengesbach, U. Kölle, and W. Oschmann, "Two Routes to Complex Derivatives of Borole," *Angewandte Chemie International Edition* 16 (1977): 42–43, https://doi.org/10.1002/anie.197700421.

32. G. E. Herberich, B. Buller, B. Hessner, and W. Oschmann, "Derivative des Borols : II. Pentaphenylborol: Synthese, Reduktion zum Dianion und Komplexe von Kobalt und Platin," *Journal of Organometallic Chemistry* 195 (1980): 253–259, https://doi.org/10.1016/S0022-328X(00)93308-4.

33. G. E. Herberich, B. Hessner, W. Boveleth, H. Lüthe, R. Saive, and L. Zelenka, "A Novel and General Route to (η^5-Borole) Metal Complexes: Compounds of Manganese, Ruthenium, and Rhodium," *Angewandte Chemie International Edition* 22 (1983): 996–996, https://doi.org/10.1002/anie.198309961.

34. G. E. Herberich, J. Hengesbach, G. Huttner, A. Frank, and U. Schubert, "Tripeldecker-Komplexe: III. Komplexierungsreaktionen von 1-Phenyl-4,5-dihydroborepin unter Gerüstumlagerung. Synthese und Struktur von Tripeldecker-Komplexen des Mangans und des Eisens mit 2-Ethyl-1-phenylborol als Brückenligand," *Journal of Organometallic Chemistry* 246 (1983): 141–149, https://doi.org/10.1016/0022-328X(83)80193-4.

35. G. E. Herberich, W. Boveleth, B. Hessner, D. P. J. Köffer, M. Negele, and R. Saive, "Derivative des Borols: VI. Dehydrierende Komplexierung von Borolenen mit Carbonylmetallen: (Borol)metall-Komplexe von Mangan, Eisen und Cobalt," *Journal of Organometallic Chemistry* 308 (1986): 153–166, https://doi.org/10.1016/S0022-328X(00)99531-7.

36. G. E. Herberich, B. Hessner, and R. Saive, "Derivate des Borols: VIII. (η5-Borol)cobalt-Komplexe," *Journal of Organometallic Chemistry* 319 (1987): 9–27, https://doi.org/10.1016/0022-328X(87)80343-1.

37. G. E. Herberich, B. Hessner, M. Negele, and J. A. K. Howard, "Borole Berivatives: X. Syntheses of (η5-Borole)metal Complexes via Borole Ammonia Adducts. Complexes of the Chromium Group Metals and the Crystal and Molecular Structures of Tetracarbonyl [η5-(1-Phenylborole)] Chromium and its Molybdenum Analogue," *Journal of Organometallic Chemistry* 336 (1987): 29–43, https://doi.org/10.1016/0022-328X(87)87155-3.

38. G. E. Herberich, U. Englert, M. Hostalek, and R. Laven, "Derivate Des Borols, XVI Bis(borol)Nickel-Komplexe[2)]," *Chemische Berichte* 124 (1991): 17–23, https://doi.org/10.1002/cber.19911240104.

39. D. V. Muratov, P. V. Petrovskii, Z. A. Starikova, G. E. Herberich, and A. R. Kudinov, "Rhodium-Containing Triple-Decker Complexes With a central Borole Ligand," *Journal of Organometallic Chemistry* 691 (2006): 3251–3259, https://doi.org/10.1016/j.jorganchem.2006.03.032.

40. H. Braunschweig, C.-W. Chiu, J. Wahler, K. Radacki, and T. Kupfer, "Chemical Reduction and Dimerization of 1-Chloro-2,3,4,5-Tetraphenylborole," *Chemistry - A European Journal* 16 (2010): 12229–12233, https://doi.org/10.1002/chem.201001556.

41. H. Braunschweig, C.-W. Chiu, A. Damme, et al., "Oligo(Borolyl) Benzenes—Synthesis and Properties," *Chemistry - A European Journal* 18 (2012): 14292–14304, https://doi.org/10.1002/chem.201202345.

42. C.-W. So, D. Watanabe, A. Wakamiya, and S. Yamaguchi, "Synthesis and Structural Characterization of Pentaarylboroles and Their Dianions," *Organometallics* 27 (2008): 3496–3501, https://doi.org/10.1021/om8002812.

43. V. Y. Lee, H. Sugasawa, O. A. Gapurenko, et al., "From Borapyramidane to Borole Dianion," *Journal of the American Chemical Society* 140 (2018): 6053–6056, https://doi.org/10.1021/jacs.8b03473.

44. G. E. Herberich and H. Ohst, "Derivate des Borols, V. Synthese von [1-(Diisopropylamino)borol]metall-Komplexen und das Diels-Alder-Dimere des 1-(Diisopropylamino)borols," *Chemische Berichte* 118 (1985): 4303–4313, https://doi.org/10.1002/cber.19851181103.

45. P. E. Romero, W. E. Piers, S. A. Decker, D. Chau, T. K. Woo, and M. Parvez, "η^1 Versus η^5 Bonding Modes in Cp*Al(I) Adducts of 9-Borafluorenes," *Organometallics* 22 (2003): 1266–1274, https://doi.org/10.1021/om0209935.

15213773, 2026, 33, Downloaded from https://onlinelibrary.wiley.com/doi/10.1002/anie.6667904 by Universitatsbibliothek RWTH Aachen University, Wiley Online Library on [29/10/2026]. See the Terms and Conditions (https://onlinelibrary.wiley.com/terms-and-conditions) on Wiley Online Library for rules of use; OA articles are governed by the applicable Creative Commons License

46. J. Sarcevic, T. Heitkemper, P. N. Ruth, et al., "A Donor-Supported Silavinylidene and Silylium Ylides: Boroles as a Flexible Platform for Versatile Si(II) Chemistry," *Chemical Science* 14 (2023): 5148–5159, https://doi.org/10.1039/D3SC00808H.

47. P. Tholen, Z. Dong, M. Schmidtmann, L. Albers, and T. Müller, "A Neutral η^5-Aminoborole Complex of Germanium(II)," *Angewandte Chemie International Edition* 57 (2018): 13319–13324, https://doi.org/10.1002/anie.201808271.

48. T. Heitkemper, J. Sarcevic, and C. P. Sindlinger, "A Neutral Silicon(II) Half-Sandwich Compound," *Journal of the American Chemical Society* 142 (2020): 21304–21309, https://doi.org/10.1021/jacs.0c11904.

49. J. Sarcevic, T. Heitkemper, and C. P. Sindlinger, "Borole-Based Half-Sandwich Complexes of Germanium and Tin," *Chemical Communications* 58 (2022): 246–249, https://doi.org/10.1039/D1CC06227A.

50. R. N. Grimes, W. J. Rademaker, M. L. Denniston, R. F. Bryan, and P. T. Greene, "Carboranes Containing Gallium and Indium Cage Heteroatoms. Synthesis, Molecular Structure, and Reactions," *Journal of the American Chemical Society* 94 (1972): 1865–1869, https://doi.org/10.1021/ja00761a013.

51. M. A. Bandman, C. B. Knobler, and M. F. Hawthorne, "The Synthesis and Structural Characterization of the First Gallacarborane Sandwich," *Inorganic Chemistry* 28 (1989): 1204–1206, https://doi.org/10.1021/ic00306a002.

52. N. S. Hosmane, K. J. Lu, H. Zhang, L. Jia, A. H. Cowley, and M. A. Mardones, "Chemistry of *C*-Trimethylsilyl-Substituted Main-Group Heterocarboranes. 8. Synthesis of closo-Gallacarboranes and Their Reactivity toward a Bis(bidentate) Lewis Base, 2,2'-Bipyrimidine: Crystal Structures of closo-1-(tert-C_4H_9)-1-Ga-2,3-($SiMe_3$)$_2$-2,3-$C_2B_4H_4$ and 1,1'-(2,2'-$C_8H_6N_4$)[1-(tert-C_4H_9)-1-Ga-2,3-($SiMe_3$)$_2$-2,3-$C_2B_4H_4$]$_2$," *Organometallics* 10 (1991): 963–970, https://doi.org/10.1021/om00050a031.

53. N. S. Hosmane, K.-J. Lu, H. Zhang, and J. A. Maguire, "Chemistry of C-Trimethylsilyl-Substituted Heterocarboranes. 22. Synthetic, Spectroscopic, Structural, and Bonding Studies on Half- and Full-Sandwich Gallacarboranes of 2,3- and 2,4-C_2B_4 Carborane Ligand Systems," *Organometallics* 16 (1997): 5163–5170, https://doi.org/10.1021/om970555b.

54. J.-D. Lee, S.-K. Kim, T.-J. Kim, et al., "Dicarbollylamine Ligand as a Tunable Template for σ,σ- and π,σ-Bonding Modes: Syntheses, Structures, and Theoretical Studies of η^5:H^1-Coordinated Constrained-Geometry Group 13 Metal Complexes," *Journal of the American Chemical Society* 130 (2008): 9904–9917, https://doi.org/10.1021/ja802163q.

55. The ESI contains NMR monitoring plots for the progressing formation of **2** including the respective signal sets of the intermediate. It is unlikely that the ^{7}Li signal at $\delta = -3$ ppm stems from residual coupling product Cp*Li solvates as this reveals expectably more pronounced highfield-shifted signal from strong ring-current effects of Cp*-.

56. The range between +300 and −700 ppm was screened. The computationally predicted chemical shift (PBE0-D3BJ/def2-TZVP) was calculated to be round −290 ppm.

57. D. Loos and H. Schnöckel, "(Cyclopentadienyl)-Gallium(I)-Verbindungen," *Journal of Organometallic Chemistry* 463 (1993): 37–40, https://doi.org/10.1016/0022-328X(93)83395-C.

58. O. Kysliak, H. Görls, and R. Kretschmer, "Cooperative Bond Activation by a Bimetallic Main-Group Complex," *Journal of the American Chemical Society* 143 (2021): 142–148, https://doi.org/10.1021/jacs.0c12166.

59. C. Helling, J. C. Farmer, C. Wölper, R. Kretschmer, and S. Schulz, "Bond Activation by a Bimetallic Ga^I Complex: Avenue to Intermetallic Compounds," *Organometallics* 42 (2023): 72–80, https://doi.org/10.1021/acs.organomet.2c00521.

60. C. Helling, L. Döhler, O. Kysliak, et al., "Metal–metal Cooperativity Boosts Lewis Basicity and Reduction Properties of the Bis(Gallanediyl)^{Cy} L_2 Ga_2," *Dalton Transactions* 53 (2024): 4922–4929, https://doi.org/10.1039/D4DT00172A.

61. A. Nagel, M. Neubauer, D. L. Miller, P. Köhler, R. Tonner-Zech, and R. Kretschmer, "Bimetallic Activation of SF_6 by a Bis(Gallylene)," *Inorganic Chemistry* 64 (2025): 24948–24957, https://doi.org/10.1021/acs.inorgchem.5c04924.

62. A. Nagel, M. Neubauer, P. Köhler, T. Rüffer, C. Hering-Junghans, and R. Kretschmer, "Gallium/Group 15 Heterocycles Derived From a Bis(gallylene)," *European Journal of Inorganic Chemistry* 29 (2026): e202500538, https://doi.org/10.1002/ejic.202500538.

63. B. Buchin, C. Gemel, T. Cadenbach, R. Schmid, and R. A. Fischer, "The $[Ga_2(C_5Me_5)]^+$ Ion: Bipyramidal Double-Cone Structure and Weakly Coordinated, Monovalent Ga^+," *Angewandte Chemie International Edition* 45 (2006): 1074–1076, https://doi.org/10.1002/anie.200503028.

64. M. Schorpp and I. Krossing, "Stack by Stack: From the Free Cyclopentadienylgermanium Cation via Heterobimetallic Main-Group Sandwiches to Main-Group Sandwich Coordination Polymers," *Chemistry - A European Journal* 26 (2020): 14109–14117, https://doi.org/10.1002/chem.202002932.

65. B. Buchin, C. Gemel, T. Cadenbach, I. Fernández, G. Frenking, and R. A. Fischer, ""Naked" Ga^+ and In^+ as Pure Acceptor Ligands: Structure and Bonding of $[GaPt(GaCp^*)_4][BAr^F]$," *Angewandte Chemie International Edition* 45 (2006): 5207–5210, https://doi.org/10.1002/anie.200601007.

66. A. D. Becke, "Density-functional Exchange-energy Approximation With Correct Asymptotic Behavior," *Physical Review A* 38 (1988): 3098–3100, https://doi.org/10.1103/PhysRevA.38.3098.

67. J. P. Perdew and W. Yue, "Accurate and Simple Density Functional for the Electronic Exchange Energy: Generalized Gradient Approximation," *Physical Review B* 33 (1986): 8800–8802, https://doi.org/10.1103/PhysRevB.33.8800.

68. F. Neese, "The ORCA Program System," *WIREs Computational Molecular Science* 2 (2012): 73–78, https://doi.org/10.1002/wcms.81.

69. F. Neese, "Software Update: The ORCA Program System, Version 4.0," *WIREs Computational Molecular Science* 8 (2018): e1327, https://doi.org/10.1002/wcms.1327.

70. F. Weigend and R. Ahlrichs, "Balanced Basis Sets of Split Valence, Triple Zeta Valence and Quadruple Zeta Valence Quality for H to Rn: Design and Assessment of Accuracy," *Physical Chemistry Chemical Physics* 7 (2005): 3297–3305, https://doi.org/10.1039/b508541a.

71. F. Weigend, "Accurate Coulomb-fitting Basis Sets for H to Rn," *Physical Chemistry Chemical Physics* 8 (2006): 1057–1065, https://doi.org/10.1039/b515623h.

72. S. Grimme, S. Ehrlich, and L. Goerigk, "Effect of the Damping Function in Dispersion Corrected Density Functional Theory," *Journal of Computational Chemistry* 32 (2011): 1456–1465, https://doi.org/10.1002/jcc.21759.

73. E. Leiner and M. Scheer, "Cp*GaCl2 and Cp*2GaCl (Cp*=η1-C5Me5) as Starting Materials for Novel Group 13 Element Complexes," *Journal of Organometallic Chemistry* 646 (2002): 247–254, https://doi.org/10.1016/S0022-328X(01)01315-8.

74. I.-A. Bischoff, B. Morgenstern, M. Zimmer, and A. Schäfer, "Heavy Pentaisopropylcyclopentadienyltriylenes and Their Heterobimetallic Complexes," *Angewandte Chemie International Edition* 64 (2025): e202419688, https://doi.org/10.1002/anie.202419688.

75. P. Jutzi, B. Neumann, G. Reumann, and H.-G. Stammler, "Pentamethylcyclopentadienylgallium (Cp*Ga): Alternative Synthesis and Application as a Terminal and Bridging Ligand in the Chemistry of Chromium, Iron, Cobalt, and Nickel," *Organometallics* 17 (1998): 1305–1314, https://doi.org/10.1021/om970913a.

76. R. S. Ghadwal, H. W. Roesky, S. Merkel, and D. Stalke, "Ambiphilicity of Dichlorosilylene in a Single Molecule," *Chemistry: A European Journal* 16 (2010): 85–88, https://doi.org/10.1002/chem.200902930.

77. N. Geibel, L. Bührmann, L. Albers, M. Schmidtmann, A. Weiz, and T. Müller, "Germaaluminocenes—Masked Heterofulvenes," *Angewandte Chemie International Edition* 63 (2024): e202403652, https://doi.org/10.1002/anie.202403652.

15213773, 2026, 33, Downloaded from https://onlinelibrary.wiley.com/doi/10.1002/anie.6667904 by Universitatsbibliothek RWTH Aachen University, Wiley Online Library on [29/10/2026]. See the Terms and Conditions (https://onlinelibrary.wiley.com/terms-and-conditions) on Wiley Online Library for rules of use; OA articles are governed by the applicable Creative Commons License

78. H. Arp, J. Baumgartner, C. Marschner, P. Zark, and T. Müller, "Dispersion Energy Enforced Dimerization of a Cyclic Disilylated Plumbylene," *Journal of the American Chemical Society* 134 (2012): 6409–6415, https://doi.org/10.1021/ja300654t.

79. A. Hofmann, C. Pranckevicius, T. Tröster, and H. Braunschweig, "Aluminum(I)/Boron(III) Redox Reactions," *Angewandte Chemie International Edition* 58 (2019): 3625–3629, https://doi.org/10.1002/anie.201813619.

80. R. J. Wright, A. D. Phillips, S. Hino, and P. P. Power, "Synthesis and Reactivity of Dimeric Ar′TlTlAr′ and Trimeric $(Ar''Tl)_3$ (Ar′, Ar′′ = Bulky Terphenyl Group) Thallium(I) Derivatives: Tl(I)−Tl(I) Bonding in Species Ligated by Monodentate Ligands," *Journal of the American Chemical Society* 127 (2005): 4794–4799, https://doi.org/10.1021/ja0432259.

81. N. J. Hardman, P. P. Power, J. D. Gorden, C. L. B. Macdonald, and A. H. Cowley, "Gallium–Boron Donor–Acceptor Bonds," *Chemical Communications* 2001 (2001): 1866–1867, https://doi.org/10.1039/b106599h.

82. N. J. Hardman, R. J. Wright, A. D. Phillips, and P. P. Power, "Structures, Bonding, and Reaction Chemistry of the Neutral Organogallium(I) Compounds $(GaAr)_n$ (n = 1 or 2) (Ar = Terphenyl or Related Ligand): an Experimental Investigation of Ga−Ga Multiple Bonding," *Journal of the American Chemical Society* 125 (2003): 2667–2679, https://doi.org/10.1021/ja028579j.

83. K. Yurkerwich and G. Parkin, "Catenated Gallium Compounds Supported by a Tris(pyrazolyl)Hydroborato Ligand," *Journal of Cluster Science* 21 (2010): 225–234, https://doi.org/10.1007/s10876-010-0314-x.

84. C. Schenk, R. Köppe, H. Schnöckel, and A. Schnepf, "A Convenient Synthesis of Cyclopentadienylgallium—The Awakening of a Sleeping Beauty in Organometallic Chemistry," *European Journal of Inorganic Chemistry* 2011 (2011): 3681–3685, https://doi.org/10.1002/ejic.201100672.

85. V. A. Dodonov, A. G. Morozov, R. V. Rumyantsev, et al., "Synthesis and ε-Caprolactone Polymerization Activity of Electron-Deficient Gallium and Aluminum Species Containing a Charged Redox-Active Dpp-Bian Ligand," *Inorganic Chemistry* 58 (2019): 16559–16573, https://doi.org/10.1021/acs.inorgchem.9b02592.

86. P. Jutzi, B. Neumann, G. Reumann, L. O. Schebaum, and H.-G. Stammler, "Lewis Acid−Base Adducts of Pentamethylcyclopentadienylgallium With Trivalent Group 13-Element Compounds," *Organometallics* 20 (2001): 2854–2858, https://doi.org/10.1021/om010132g.

87. J. T. Boronski, A. E. Crumpton, L. L. Wales, and S. Aldridge, "Diberyllocene, a Stable Compound of Be(I) With a Be–Be Bond," *Science* 380 (2023): 1147–1149, https://doi.org/10.1126/science.adh4419.

88. J. T. Boronski, A. E. Crumpton, A. F. Roper, and S. Aldridge, "A Nucleophilic Beryllyl Complex via Metathesis at $[Be–Be]^{2+}$," *Nature Chemistry* 16 (2024): 1295–1300, https://doi.org/10.1038/s41557-024-01534-9.

89. I. Resa, E. Carmona, E. Gutierrez-Puebla, and A. Monge, "Decamethyldizincocene, a Stable Compound of Zn(I) With a Zn-Zn Bond," *Science* 305 (2004): 1136–1138, https://doi.org/10.1126/science.1101356.

90. A. Grirrane, I. Resa, A. Rodriguez, et al., "Zinc−Zinc Bonded Zincocene Structures. Synthesis and Characterization of Zn_2 (η^5-C_5Me_5)$_2$ and Zn_2 (η^5-C_5Me_4Et)$_2$," *Journal of the American Chemical Society* 129 (2007): 693–703, https://doi.org/10.1021/ja0668217.

91. I.-A. Bischoff, S. Danés, P. Thoni, et al., "A Lithium–Aluminium Heterobimetallic Dimetallocene," *Nature Chemistry* 16 (2024): 1093–1100, https://doi.org/10.1038/s41557-024-01531-y.

92. A. K. Saxena, H. Zhang, J. A. Maguire, N. S. Hosmane, and A. H. Cowley, "Surprising Formation of a Carborane-Substituted Digallane," *Angewandte Chemie International Edition* 34 (1995): 332–334, https://doi.org/10.1002/anie.199503321.

93. D. S. Brown, A. Decken, and A. H. Cowley, "Gallium-Containing 6π-Electron Ring Systems," *Journal of the American Chemical Society* 117 (1995): 5421–5422, https://doi.org/10.1021/ja00124a050.

94. W. Uhl, T. Spies, and R. Koch, "Di(μ-acetato)dialkyldigallium as Starting Compound for the Facile Syntheses of Digallium Derivatives Containing Bridged or Terminally Co-ordinated GaGa Single Bonds," *Journal of the Chemical Society, Dalton Transactions* (1999): 2385–2392, https://doi.org/10.1039/A903437D.

95. Y. Zhang, Y. Chi, J. Wei, et al., "Aromatic Tetralithiodigalloles With a Ga–Ga Bond: Synthesis and Structural Characterization," *Organometallics* 36 (2017): 2982–2986, https://doi.org/10.1021/acs.organomet.7b00447.

96. A. V. Protchenko, J. Urbano, J. A. B. Abdalla, et al., "Electronic Delocalization in Two and Three Dimensions: Differential Aggregation in Indium "Metalloid" Clusters," *Angewandte Chemie International Edition* 56 (2017): 15098–15102, https://doi.org/10.1002/anie.201708496.

97. Z. Feng, Y. Fang, H. Ruan, Y. Zhao, G. Tan, and X. Wang, "Stable Radical Cation and Dication of an N-Heterocyclic Carbene Stabilized Digallene: Synthesis, Characterization and Reactivity," *Angewandte Chemie International Edition* 59 (2020): 6769–6774, https://doi.org/10.1002/anie.202000051.

98. J. T. Boronski, M. P. Stevens, B. van IJzendoorn, A. C. Whitwood, and J. M. Slattery, "Insights Into the Composition and Structural Chemistry of Gallium(I) Triflate," *Angewandte Chemie International Edition* 60 (2021): 1567–1572, https://doi.org/10.1002/anie.202010837.

99. A. Barthélemy, H. Scherer, H. Weller, and I. Krossing, "How Long Are Ga⇆Ga Double Bonds and Ga–Ga Single Bonds in Dicationic Gallium Dimers?," *Chemical Communications* 59 (2023): 1353–1356, https://doi.org/10.1039/D2CC06377H.

100. The experimental IR spectrum (see SI) fits the computationally predicted IR of **6** and does not reveal any potential Ga-H stretching frequencies. A computationally optimized $[(borole)GaH]_2$ would reveal much larger Ga-Ga distances (ca. 2.78 Å) than those observed by single crystal X-ray diffraction (2.37 Å). Moreover, a high resolution X-ray diffraction dataset (down to 0.45 Å) was obtained. No residual electron density for putative bridging hydrides are observed see SI.

101. C. Ganesamoorthy, S. Loerke, C. Gemel, et al., "Reductive Elimination: A Pathway to Low-valent Aluminium Species," *Chemical Communications* 49 (2013): 2858–2860, https://doi.org/10.1039/c3cc38584a.

102. The computationally (BP86-D3BJ/def2TZVPP CPCM = Benzene) calculated ΔG^{298K} amounts to only –0.3 kcal mol^{-1}.

103. E. D. Glendening, C. R. Landis, and F. Weinhold, "Natural Bond Orbital Methods," *WIREs Computational Molecular Science* 2 (2012): 1–42, https://doi.org/10.1002/wcms.51.

104. E. D. Glendening, J. K. Badenhoop, A. E. Reed, et al., NBO 7.0 (Theoretical Chemical Institute, University of Wisconsin Madison, 2018).

105. M. P. Mitoraj, A. Michalak, and T. Ziegler, "A Combined Charge and Energy Decomposition Scheme for Bond Analysis," *Journal of Chemical Theory and Computation* 5 (2009): 962–975, https://doi.org/10.1021/ct800503d.

106. P. Jerabek, P. Schwerdtfeger, and G. Frenking, "Dative and Electron-Sharing Bonding in Transition Metal Compounds," *Journal of Computational Chemistry* 40 (2019): 247–264, https://doi.org/10.1002/jcc.25584.

107. F. M. Bickelhaupt and E. J. Baerends, "Kohn-Sham Density Functional Theory: Predicting and Understanding Chemistry," in *Reviews in Computational Chemistry*, ed. K. B. Lipkowitz and D. B. Boyd (Wiley, 2000), 1–86.

108. E. J. Baerends, T. Ziegler, A. J. Atkins, et al., ADF2022, SCM (Theoretical Chemistry, Vrije Universiteit, 2022), https://www.scm.com.

109. P. Dabringhaus and I. Krossing, "From Mixed Group 13 Cations $[M(AlCp^*)_3]^+$ (M = Ga/In/Tl) to an Al^+ Cluster," *Chemical Science* 13 (2022): 12078–12086, https://doi.org/10.1039/D2SC04637G.

110. P. Dabringhaus, J. Willrett, and I. Krossing, "Synthesis of a Low-Valent Al_4^+ Cluster Cation Salt," *Nature Chemistry* 14 (2022): 1151–1157, https://doi.org/10.1038/s41557-022-01000-4.

15213773, 2026, 33, Downloaded from https://onlinelibrary.wiley.com/doi/10.1002/anie.6667904 by Universitatsbibliothek RWTH Aachen University, Wiley Online Library on [29/10/2026]. See the Terms and Conditions (https://onlinelibrary.wiley.com/terms-and-conditions) on Wiley Online Library for rules of use; OA articles are governed by the applicable Creative Commons License

111. D. Weiss, T. Steinke, M. Winter, et al., "[(dcpe)Pt(ECp*)$_2$] (E = Al, Ga): Synthesis, Structure, and Bonding Situation of the First Aluminum(I) and Gallium(I) Complexes of Phosphine-Substituted Transition Metal Centers," *Organometallics* 19 (2000): 4583–4588, https://doi.org/10.1021/om000310q.

112. D. Weiß, M. Winter, R. A. Fischer, C. Yu, K. Wichmann, and G. Frenking, "[Pt_2(GaCp*)$_2$(μ_2-GaCp*)$_3$]: Structure and Bonding Situation of the First Homoleptic Platinum Complex With Terminal and Bridging Cp*Ga Ligands," *Chemical Communications* (2000): 2495–2496, https://doi.org/10.1039/B008133G.

113. T. Steinke, C. Gemel, M. Winter, and R. A. Fischer, "[Pd_3 (InCp*)$_4$ (μ_2-InCp*)$_4$]: Drei Linear Angeordnete Palladium-Atome in Einer Fluktuierenden Verpackung Aus Acht [Cp*In]-Liganden," *Angewandte Chemie* 114 (2002): 4955–4957, https://doi.org/10.1002/ange.200290040.

114. C. Gemel, T. Steinke, D. Weiss, M. Cokoja, M. Winter, and R. A. Fischer, "[M(GaCp*)$_4$] (M = Pd, Pt) as Building Blocks for Dimeric Homoleptic Cluster Compounds of the Type [MPt(GaCp*)$_5$]," *Organometallics* 22 (2003): 2705–2710, https://doi.org/10.1021/om021003i.

115. T. Steinke, C. Gemel, M. Winter, and R. A. Fischer, "The Clusters [M_a (ECp*)$_b$] (M=Pd, Pt; E=Al, Ga, In): Structures, Fluxionality, and Ligand Exchange Reactions," *Chemistry: A European Journal* 11 (2005): 1636–1646, https://doi.org/10.1002/chem.200400959.

116. M. Halbherr, T. Bollermann, C. Gemel, and R. A. Fischer, "Selective Oxidative Cleavage of Cp* From Coordinated GaCp*: Naked Ga^+ in [GaNi(GaCp*)$_4$]$^+$ and [(μ_2-Ga)$_n$M$_3$(GaCp*)$_6$]$^{n+}$," *Angewandte Chemie International Edition* 49 (2010): 1878–1881, https://doi.org/10.1002/anie.200905920.

117. P. Jutzi, B. Neumann, L. O. Schebaum, A. Stammler, and H.-G. Stammler, "Steric Demand of the Cp*Ga Ligand: Synthesis and Structure of Ni(Cp*Ga)$_4$ and of Cis-M(Cp*Ga)$_2$(CO)$_4$ (M = Cr, Mo)," *Organometallics* 18 (1999): 4462–4464, https://doi.org/10.1021/om990355v.

118. J. K. Schuster, J. H. Muessig, R. D. Dewhurst, and H. Braunschweig, "Reactions of Digallanes With p- and D-Block Lewis Bases: Adducts, Bis(gallyl) Complexes, and Naked Ga^+ as Ligand," *Chemistry: A European Journal* 24 (2018): 9692–9697, https://doi.org/10.1002/chem.201801471.

119. T. Cadenbach, C. Gemel, T. Bollermann, I. Fernandez, G. Frenking, and R. A. Fischer, "Organometallic Chemistry of Ga^+: Formation of an Unusual Gallium Dimer in the Coordination Sphere of Ruthenium," *Chemistry: A European Journal* 14 (2008): 10789–10796, https://doi.org/10.1002/chem.200801328.

120. Deposition Numbers 2519914 (for **A**Li$_2$(tol)$_2$), 2519919 (for **2**), 2519920 (for **3**), 2519917 (for **4**), 2519915 (for **5**), 2519916 (for **6**), 2519918 (for **7**) and 2519921 (for **8**) contain the supplementary crystallographic data for this paper. These data are provided free of charge by the joint Cambridge Crystallographic Data Centre and Fachinformationszentrum Karlsruhe Access Structures Service.

Supporting Information

Additional supporting information can be found online in the Supporting Information section.

Further supporting information, including a detailed methodological summary, synthetic procedures, spectroscopic and crystallographic evidence on the compounds, as well as computational details, is provided in the ESI file. CIF files of the structures reported have been deposited with the CCDC database (deposition numbers 2519914–2519921) [120].

Supporting File 1: anie72722-sup-0001-Data.zip.

Supporting File 2: anie72722-sup-0002-SuppMat.pdf.

15213773, 2026, 33, Downloaded from https://onlinelibrary.wiley.com/doi/10.1002/anie.666790 4 by Universitatsbibliothek RWTH Aachen University, Wiley Online Library on [29/10/2026]. See the Terms and Conditions (https://onlinelibrary.wiley.com/terms-and-conditions) on Wiley Online Library for rules of use; OA articles are governed by the applicable Creative Commons License